PROCESS MONITORING BASED ON NONLINEAR WAVELET PACKET PCA

Xiuxi Li, Junfeng Wang , Yu Qian*， and Yanbin Jiang

School of Chemical Engineering, South China University of Technology, Guangzhou, 510640, China

Abstract: For using process operational data to realize process monitoring, kinds of improved PCA are applied to cope with complexity of industrial processes. In this paper, a novel nonlinear wavelet packet PCA (NLWPPCA) method, which combines input training network with wavelet packet PCA, is proposed. Wavelet packet PCA integrates ability of PCA to de-correlate the variables by extracting a linear relationship with what of wavelet packet analysis to extract auto-correlated measurements. Then the paper gives the methodology of process monitoring based on NLWPPCA. Finally, the proposed approach is successfully applied to an eight variables nonlinear process with noise and Tennessee Eastman process for process monitoring.

Keywords: Process monitoring; Wavelet packet analysis; Principal components analysis

1. INTRODUCTION

With the increase in on-line data acquisition systems in industrial processes, the collection of process operational data is becoming routine. Then process plants are becoming data rich but information poor. There is therefore a need to extract the inherent information within the data. Data mining techniques, which mining inherent useful knowledge from kinds of databases or data warehouses, are introduced to process monitoring. Then process monitoring based on data mining is to collect raw data from time-series database or data sets, reprocess data using data reconciliation method, mine outliers and classification or clustering analyze these outliers. Principal components analysis (PCA) as an effective method of data mining techniques has been widely applied in process monitoring. However, many industrial processes exhibit significant nonlinear behaviour and industrial data is also synonymous with process measurement noise. In these cases the application of PCA is not strictly appropriate. Then many improved methods are proposed and applied. Kramer (1991) used an auto-associative neural network, trained using backpropagation to produce a nonlinear PCA. Dong and McAvoy (1994) integrated principal curves with a neural network to build a nonlinear PCA. Tan and Mavrovouniotis (1995) proposed a nonlinear PCA based on input-training neural network. Bakshi (1998) introduced the principle of multiscale PCA, which combines the attractive properties of linear PCA and wavelet analysis by computing the PCA of wavelet coefficients at each scale and then combining the results at relevant scales. Chen, et al. (1999) combined neural networks and multiscale wavelet analysis in a modified version of the adaptive resonance theory for diagnostic system development. Shao, et al. (1999) proposed a nonlinear PCA algorithm for process monitoring based on an input-training neural network and also applied wavelet denoising and non-parametric control limits. Fourie and Vaal (2000) gave an on-line nonlinear multiscale principal component analysis methodology.

Wavelet packet PCA integrates PCA and wavelet packet analysis. Wavelet packet analysis decomposes the high-frequency part further, which wavelet analysis not does, and adaptively selects relative frequency bond based on character of signal to be analyzed. To further improve denoising character of multiscale PCA, the paper describes a wavelet packet PCA, which combines the ability of PCA to decorrelate the variables by extracting a linear

* Corresponding author: +87112046, Email:ceyuqian@scut.edu.cn

relationship with that of wavelet packet analysis to extract autocorrelated measurements. Then, a novel nonlinear wavelet packet PCA is proposed by combining input-training neural network with wavelet packet. Finally, the nonlinear wavelet packet PCA will be used to analyze two simulated systems to verify its operation.

2. WAVELET PACKET PCA

In the WPPCA, signals are decomposed first using wavelet packet to get wavelet packet decomposition coefficients matrixes. Then these coefficients matrixes use PCA to confirm the retain number of principal components and compute principal components score matrixes and load matrixes. Wavelet packet coefficients are obtained by rebuilding the score matrixes and the load matrixes. These coefficients are de-noised by using wavelet packet de-noise limit method, Rebuild signals are obtained by using wavelet packet rebuild algorithm. Finally, These rebuild signals are analyzed by PCA. The steps in the WPPCA methodology are shown in Figure 1, and the detailed procedures are given as follows.

(1) For each column in data matrix, select wavelet packet function $\Psi_{j,k,n}(t)$ and wavelet packet dividing level L and compute wavelet packet decomposition coefficients $\{W_{L,0}, W_{L,1}, \ldots, W_{L,2^L-1}\}$;
(2) For each variable, use the same best full wavelet packet base algorithm to process wavelet packet decomposition tree and find best wavelet packet decomposition coefficients;
(3) Select these coefficients as column vector to build wavelet packet coefficients matrixes with different tree nodes $\{X_{L,0}, X_{L,1},\ldots,X_{L,2^L-1}\}$, the row number of these matrix is $n/2^L$ and the column number is m;
(4) For these coefficients matrixes, respectively use conventional PCA to confirm the retain number of principal components and compute principal components score matrixes $\{T_{L,0}, T_{L,1},\ldots,T_{L,2^L-1}\}$ and load matrixes $\{P_{L,0}, P_{L,1},\ldots,P_{L,2^L-1}\}$;
(5) Use retain score matrixes and load matrixes to rebuild wavelet packet coefficients matrixes $\{X'_{L,0}, X'_{L,1},\ldots,X'_{L,2^L-1}\}$;
(6) For each column in $\{X'_{L,0}, X'_{L,1},\ldots,X'_{L,2^L-1}\}$, combines corresponding column vectors to get rebuild wavelet packet coefficients;
(7) For these coefficients, respectively use wavelet packet de-noise limit method to process these coefficients and get de-noising coefficients;
(8) Use wavelet packet rebuild algorithm to get each variable samples $\{x'_1, x'_2,\ldots,x'_m\}$;
(9) Build new data matrix X' and use PCA to select the retain number of principal components and compute score matrix T' and load matrix P'.

The WPPCA combines the ability of PCA to de-correlate the variables by extracting a linear relationship with that of wavelet packet analysis to extract auto-correlated measurements.

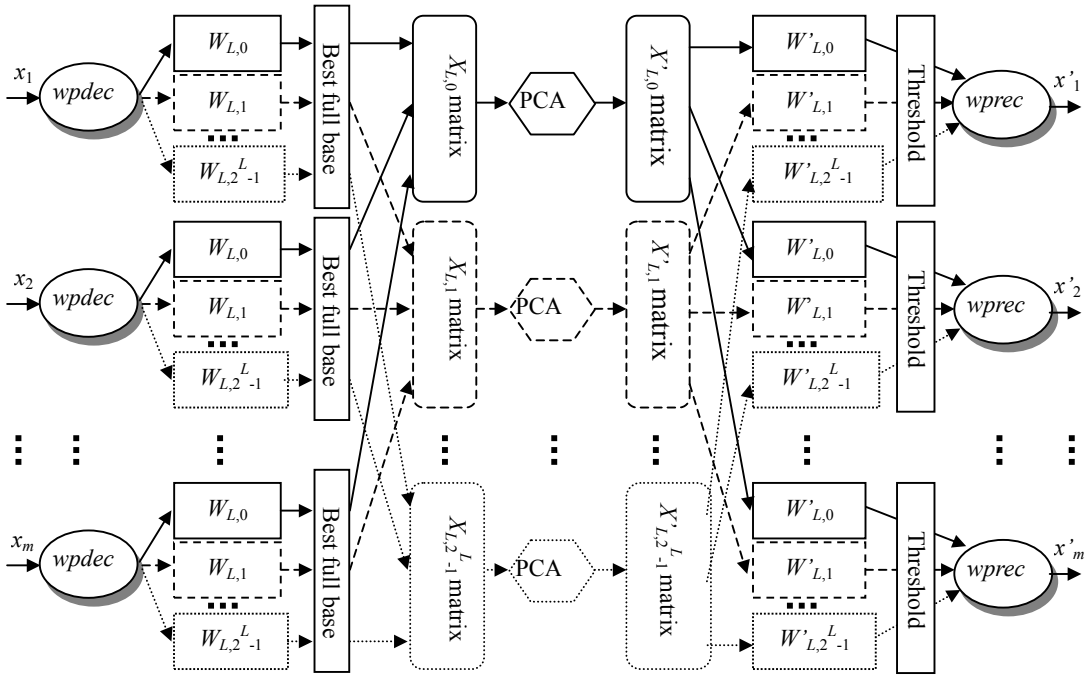

Figure 1 Methodology of wavelet packet PCA

3. NONLINEAR WAVELET PACKET PCA

Nonlinear PCA is an extension of linear PCA. Nonlinear PCA can extract both linear and nonlinear correlations, while PCA identifies linear correlations between process variables. Neural networks have long been recognized as a useful tool for extracting features from highly nonlinear data. Some researchers have proposed different approaches based on kinds of neural networks. Malthouse (1998) discussed these approaches and recommended the techniques developed from the principal curve method and the input-training network to overcome the continuous function projection constraint. The nonlinear wavelet packet PCA (NLWPPCA) method proposed in this paper is based upon the input-training neural network (IT-net). In the IT-net each data input pattern is not fixed but adjusted in conjunction with the internal network parameters to reproduce a corresponding output pattern using the steepest gradient descent optimization rule. In the approach, the process observation data are defined as the output layer pattern and the nonlinear principal scores are identified from the input layer. The architecture of the IT-net is shown in Figure 2.

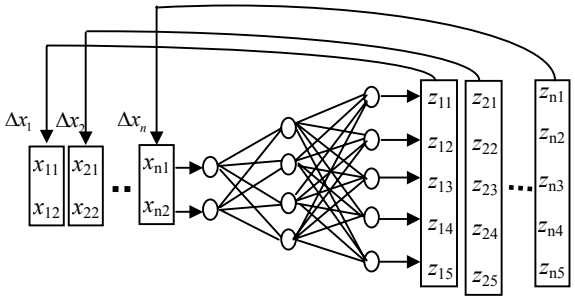

Figure 2 Structure of IT-net

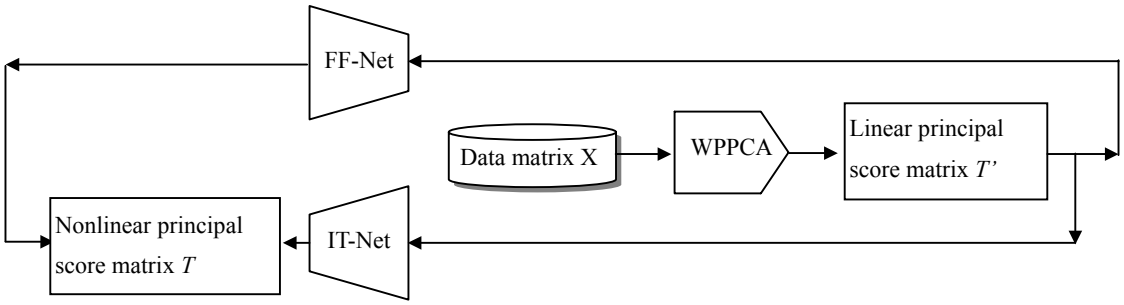

Figure 3 Methodology of nonlinear wavelet packet PCA

The NLWPPCA enables both nonlinear characters and noise characters to be analyzed. Figure 3 illustrates the NLWPPCA methodology. The implement steps of the NLWPPCA algorithm is as followed:Collect normal operation data matrix X;

(1) For each column in X, use wavelet packet PCA algorithm to compute linear principal scores matrix T' and principal loads matrix P';
(2) Let linear principal scores matrix T' as the IT-net output layer pattern, let nonlinear principal scores matrix T as the IT-net input layer pattern, select input layer nodes k and determine hidden layer nodes q and other network initial values;
(3) Use extend backpropagation algorithm to optimize network parameters and input values, then get the IT-net model $F(.)$;
(4) Let the IT-net input layer values, which be trained, as the forward feedback neural network output layer, let linear principal scores matrix T' as the forward feedback neural network (FF-net) input layer, and select similar structure as the IT-net;
(5) Use backpropagation algorithm to train the parameters, then get the FF-net model $G(.)$;
(6) Determine the nonlinear principal scores matrix T, load matrix P, and get the NLWPPCA model as $X=F(T)P^{T}+E$, where E is an error matrix.

4 PROCESS MONITORING BASED ON NLWPPCA

Algorithm implement of process monitoring based on NLWPPCA is illustrated in Figure 4. It includes two parts: off-line model determination and on-line process monitoring. Where off-line model determination includes: select best full wavelet packet base, select appropriate denoising threshold, determine the retain principal components number, compute linear principal scores matrix and loads matrix, determine the IT-net structure and initial parameters, use extend backpropagation algorithm to get nonlinear principal scores matrix, train the forward network to get the NLWPPCA model, determine statistical value limitation to monitor process. Where on-line process monitoring includes: reprocess real-time operation data to input the normal NLWPPCA model, compute each statistical value SPE and T^2, compare these values with the corresponding thresholds, determine abnormal situation.

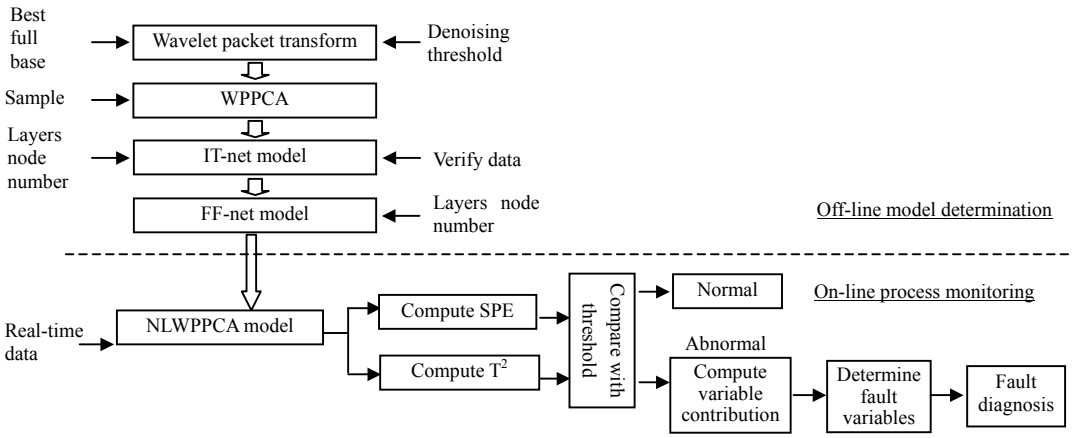

Figure 4 Algorithm of process monitoring based on NLWPPCA

5. CASE STUDY

In this Section, the proposed process monitoring based on NLWPPCA is demonstrated and tested by applying in an eight variables nonlinear process with noise and a recognized chemical process tested base Tennessee Eastman process. We will demonstrate the use of NLWPPCA approach for nonlinear monitoring purposes first with respect to a simple multivariate process as well as with the much more complex and realistic Tennessee Eastman process.

5.1 An eight variables nonlinear process with noise

Consider the following process:

$$\begin{cases} x_1=8+0.1*randn(n,1)+0.8*wnoise; \\ x_2=11+0.2*randn(n,1)+0.8*wnoise; \\ x_3=17+0.3*randn(\mathrm{n},1)+0.8*wnoise; \\ x_4=5+((-1.3*x_1^3+0.2*x_2^2)/(x_2*x_3))+0.8*wnoise; \\ x_5=120+0.8*(-3.8*x_1^2+0.8*x_2^2+0.9*x_3*x_4) \\ \quad +0.8*wnoise; \\ x_6=5+x_2-0.3*x_3+0.8*wnoise; \\ x_7=-x_1+0.8*x_2+x_4+0.8*wnoise; \\ x_8=x_2+x_3+0.8*wnoise; \end{cases}$$

where *wnoise* is a white noise with zero mean and variance 1. 1000 samples are selected as normal operation data for analysis. The initial data matrix consists of as follow:

$X=[x_1^{\mathrm{T}}\ x_2^{\mathrm{T}}\ x_3^{\mathrm{T}}\ x_4^{\mathrm{T}}\ x_5^{\mathrm{T}}\ x_6^{\mathrm{T}}\ x_7^{\mathrm{T}}\ x_8^{\mathrm{T}}]$

For data matrix X, use the proposed NLWPPCA algorithm to build off-line model. Where structure of the IT-net is 1-3-2, and hidden layer function is Sigmoid function. The IT-net is trained by extend Levenberg-Marquardt (LM) algorithm. When train step is 56, train error is 0.005. Similar, select structure of the FF-net is 2-3-1 and use LM algorithm to train the FF-net. When train step is 18, the error is 0.005. Determine the statistical limitation: SPE_a=0.1234, T^2_a=6.0060. The NLWPPCA model is used to monitor 200 real-time samples of the eight variables nonlinear process. To verify performance of monitoring, introduces mean error disturbance at 160 sample time and cancels it at 180. The process real-time trend is illustrated in Figure 5. Figure 6 shows the SPE plot and T^2 plot.

The relationship between the first principal component and the second one is shown in Figure 7. Figure 8 describes the contribution plot of the first and the second principal component. From Figure 5, it is not easy to identify the process operational situation because of nonlinear character. However, from SPE plot, SPE values before 160 times step is clearly below the SPE limitation and out of control after 160. So, SPE plot successfully finds the abnormity. Similarly, T^2 plot also finds the abnormity. From scores plot, finds some outliers away from the clustering points, which directly shows the trend. In addition, some projection points are overlapped for wavelet packet denoising. Figure 8 shows that contribution of the second and 7th variables to the first pc is biggish and contribution of the second, 5th and 7th variables to the second pc is biggish. Then, it is inferred that the abnormity is brought by the second, 5th and 7th variables. The conclusion is consistent with process model. The simulation illustrates the proposed approach is valid for nonlinear process with noise monitoring.

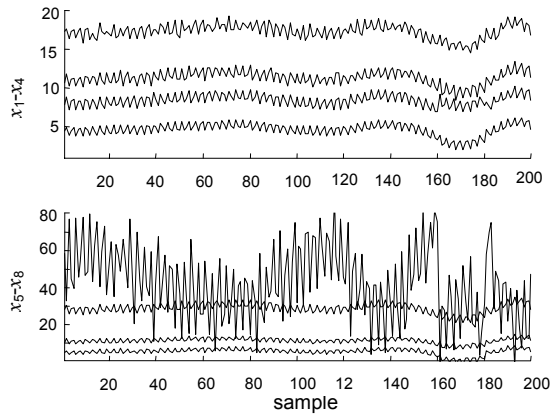

Figure 5 Real-time trends with mean error

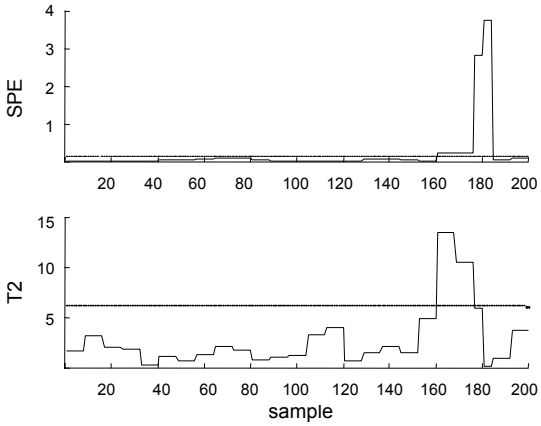

Figure 6 SPE and T^2 plots with mean error

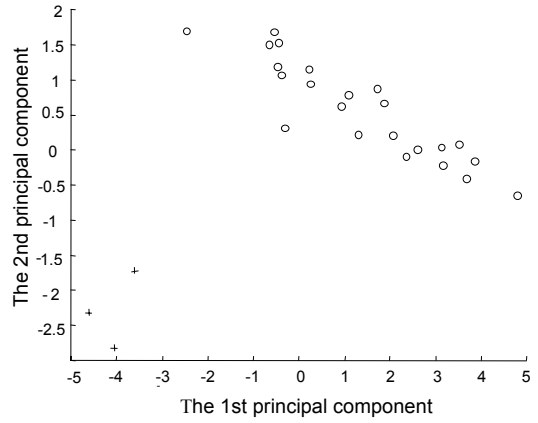

Figure 7 Scores plot with mean error

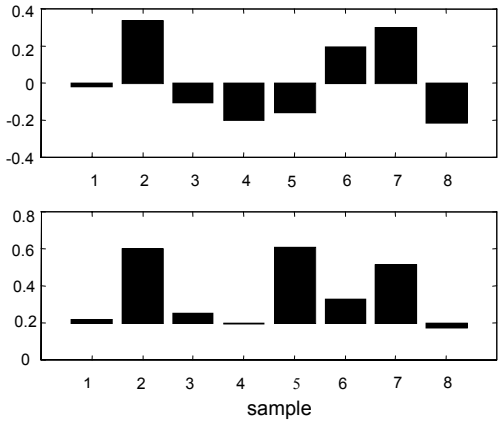

Figure 8 Contribution plot with mean error

5.2 Tennessee Eastman process

Table 1 Process disturbance

Case	Disturbance	Type
IDV(1)	A/C feed ratio, B composition constant	Step
IDV(2)	B composition, A/C ratio constant	Step
IDV(3)	D feed temperature	Step
IDV(4)	Reactor cooling water inlet temperature	Step
IDV(5)	Condenser cooling water inlet temperature	Step
IDV(6)	A feed loss	Step
IDV(7)	C header pressure loss – reduced availability	Step
IDV(8)	A, B, C feed composition	Random
IDV(9)	D feed temperature	Random
IDV(10)	C feed temperature	Random
IDV(11)	Reactor cooling water inlet temperature	Random
IDV(12)	Condenser cooling water inlet temperature	Random
IDV(13)	Reaction kinetics	Slow drift
IDV(14)	Reactor cooling water valve	Sticking
IDV(15)	Condenser cooling water valve	Sticking
IDV(16)	Unknown	Unknown

Tennessee Eastman process, which was developed by Downs and Vogel (1993), consists of five major unit operations: a reactor, a condenser, a vapor-liquid separator, a recycle compressor, and a product stripper. The process has 41 measurements, including 22 continuous process measurements and 19 composition measurements, and 12 manipulated variables. Some disturbances are programmed for researching the characteristics of the control system, listed in Table 1.

The reference set contains 1000 samples from normal operation with a sampling interval of 3 min. A NLWPPCA model is developed from the data matrix. Nine principal components are selected, which capture 97.7% of the variation in the reference set. The control limits shown in every plot correspond approximately to the 95% confidence region, which is determined by using the methodology presented by Nomikos and MacGregor:

SPE_a=7.1509, T^2_a=75.0008.

The simulation is run under the first disturbance IDV[1], which is loaded at the 300th time step. SPE plot and T^2 plot are shown in Figure 9. From these plots, disturbance is quickly and easily detected. Figure 10 shows the scores plot. The figure clearly

illustrates that process projection points are away from the normal situation. This result shows that for the TE process the proposed NLWPPCA will get well effect in process monitoring.

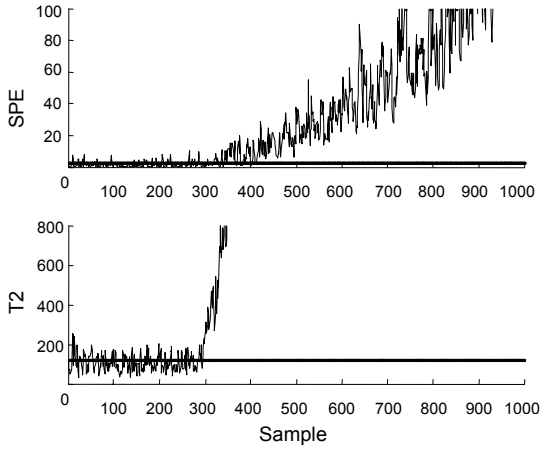

Figure 9 SPE plot and T^2 plot for IDV[1]

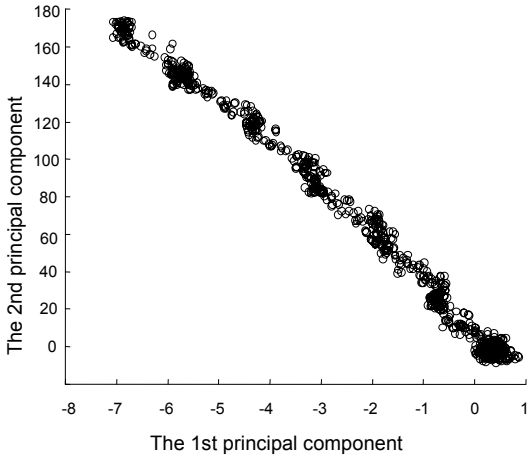

Figure 10 Scores plot for IDV[1]

6. CONCLUSIONS

In this paper, a nonlinear wavelet packet PCA approach has been proposed for process monitoring. The advantage of this method is that both linear and nonlinear correlations can be extracted from the process data with noise. Heavy noise and data spikes in the industrial data sets were first eliminated through wavelet packet denoising method. Whilst, input-training neural network was introduced to extract nonlinear character in industrial processes. The results of the application of the NLWPPCA algorithm to an eight nonlinear process and TE process demonstrate the improved performance over that of linear methods for fault detection.

ACKNOWLEDGMENTS

Financial support from the National Natural Science Foundation of China (No. 29976015), the China Excellent Young Scientist Fund, China Major Basic Research Development Program (G20000263), and the Excellent Young Professor Fund from the Education Ministry of China are gratefully acknowledged.

REFERENCES

Bakshi, B.R. (1998). Multiscale PCA with application to multivariate statistaical process monitoring. *American Institute of Chemical Engineering Journal*, 44(7),1596.

Chen, B.H., X.Z. Wang, S.H. Yang, and C. McGreavy, (1999). Application of wavelets and neural networks to diagnostic system development. Part 1. Feature extraction. *Computers & Chemical Engineering*,23,899.

Dong, D. and T.J. McAvoy, (1994). Non-linear principal component analysis based on principal curve and neural networks. *Computers & Chemical Engineering*, 20(1),65-78.

Downs, J.J. and E.F. Vogel, (1993). A plant-wide industrial process control problem. *Computer & Chemica. Engineering,17*, 245-255.

Fourie, S.H. and P.de. Vaal, (2000). Advanced process monitoring using an on-line non-linear multiscale principal component analysis methodology. *Computers & Chemical Engineering*, 24(2000)755-760.

Kramer, M. A. (1991). Non-linear principal component analysis using autoassociative neural networks. *A.I.Ch.E. Journal*, 37(2),233-243.

Ku, W., R. Storer, and C. Georgakis, (1995). Disturbance detection and isolation by dynamic principal component analysis. *Chemometrics and Intelligent Lab. Systems 30*, 179-196.

Lin, Weilu, Y. Qian, and X.X. Li, (2000). Nonlinear dynamic principal component analysis for on-line process monitoring and diagnosis. *Computer & Chemical Engineering 24*, 423-429.

Malthouse, E.C. (1998). Limitations of non-linear PCA as performed with generic neural networks. *IEEE Transactions on Neural Networks*, 9(1),165-173.

Shao, R., F. Jia, E.B. Martin, and A.J. Morris, (1999). Wavelets and non-linear principal components analysis for process monitoring. *Control Engineering Practice*, 7,865.

Tan, S., and M.L. Mavrovouniotis, (1995). Reducing data dimensionality through optimizing neural network inputs. *A.I.Ch.E. Journal*, 41(6), 1471-148.

APPLICATION OF STATISTICAL PROCESS MONITORING WITH EXTERNAL ANALYSIS TO AN INDUSTRIAL MONOMER PLANT

Tetsuhiko Yamamoto [*] **Akirou Shimameguri** [*]
Morimasa Ogawa [**] **Iori Hashimoto** [***] **Manabu Kano** [***]

[*] *Mitsubishi Chemical Corporation, Ibaraki 314-0102, Japan*
[**] *Mitsubishi Chemical Corporation, Okayama 712-8054, Japan*
[***] *Kyoto University, Kyoto 606-8501, Japan*

Abstract: The main objective of this industry-university collaboration is to develop an on-line process monitoring system that can detect a particular malfunction in an industrial monomer plant. The most serious malfunction is a blockage caused by an accumulation of polymers inside a cooling unit. Since the blockage requires shutdown maintenance, it is crucial to detect its symptom as early as possible and properly adjust the operating condition to avoid further polymer accumulation. The developed on-line monitoring system can detect the symptom of the blockage by using multivariate statistical process control, distinguish it from normal changes in operating conditions by using external analysis, and persuade operators to take appropriate action.

Keywords: process monitoring, fault detection, fault diagnosis, statistical process control, principal component analysis, external analysis, industrial application

1. INTRODUCTION

Long-term stable operation is becoming increasingly important in the chemical industry, because 1) a trouble shutdown of one plant inflicts a heavier loss on the company as production sites become more consolidated, and 2) plant managers have to get the best out of existing equipments and maximize the production efficiency. To achieve long-term efficient operation, one needs to recognize that:

- It seems impossible to entirely avoid troubles due to process upsets or equipment malfunction.
- Unexpected trouble may happen at an unexpected location during a high load operation that has never been experienced.
- The integration of operating rooms and the deployment of advanced process control systems reduce the number of operators; each operator's responsibilities have increased.

In modern chemical plants, operators must monitor a large number of process variables one after another for safe operation. Since measured process variables are highly correlated, it is difficult for operators to detect every fault without monitoring the correlation between process variables. A more difficult task than fault detection is to identify a real cause of the fault and to take prompt and appropriate action. To support operators, automation of process monitoring is greatly desired in the industry.

Multivariate statistical process control (MSPC) has been investigated as a data-based technique for multivariable process monitoring (Kresta et al., 1991; Kourti and MacGregor, 1995; Ku et al., 1995; Kano et al., 2002). MSPC is based on chemometric techniques such as

principal component analysis (PCA) and partial least squares (PLS). PCA is a tool for data compression and information extraction; it finds linear combinations of variables that describe major trends in a data set. On the other hand, PLS relates output variables to latent variables, which are given as linear combinations of input variables. A typical application of PLS in the chemical industry is to estimate product quality from measurable variables (Kano et al., 2000). These chemometric techniques are very useful for modeling and monitoring chemical processes where a great number of measured variables are highly correlated. Many researchers and practitioners have investigated MSPC to extract useful information from process data and use it for process monitoring.

In conventional SPC, a process is assumed to be operated in a particular steady state, and deviations of measurements from their steady-state values are used for monitoring. However, operating conditions cannot be constant in many processes due to production rate adjustments, product grade transitions, and so on. Therefore, it is crucial to develop a new SPC method that can cope with changes in operating conditions. In order to develop a new monitoring system for distinguishing between faults and normal changes in operating conditions, external analysis was proposed and integrated with MSPC (Kano et al., 2003).

In the present work, an on-line monitoring system is developed to detect a blockage, caused by an accumulation of polymers, in an industrial monomer plant. Since the blockage requires shutdown maintenance, it is crucial to detect its symptom as early as possible and properly adjust the operating condition for avoiding further polymer accumulation.

2. MSPC WITH EXTERNAL ANALYSIS

In the present work, changes in operating conditions, which should be distinguished from faults, are assumed to be given from the outside of a process as changes in a feed flow rate, set-points of controllers, and so on. Thus, variables that are used for monitoring can be classified into two groups. The first group consists of variables representing operating conditions such as a feed flow rate and a set-point, hereafter referred to as external variables. The second group consists of variables affected by external variables and other unmeasured disturbances. Those variables are referred to as main variables. Changes in external variables are not faults. Therefore, both the changes in external variables and their influence on main variables should be distinguished from faults. To achieve this goal, operation data of main variables are decomposed into two parts: one is a part explained by external variables, and the other is a part not explained by them. As a result, the influence of changes in external variables can be removed from operation data. This technique is called external analysis and it can be integrated with any SPC method (Kano et al., 2003).

In this section, it is briefly shown that the external analysis can be used for removing the influence of external variables from operation data and it can be integrated with PCA-based SPC.

2.1 *External Analysis*

Consider a data matrix $\boldsymbol{X} \in \Re^{k \times m}$, where k and m are the number of samples and that of variables, respectively. For simplicity, each variable is assumed to be normalized. When m_g of m variables are classified as external variables and $m_h (= m - m_g)$ are main variables, the data matrix is described as

$$\boldsymbol{X} = \left[\boldsymbol{H} \;\; \boldsymbol{G} \right] \tag{1}$$

where $\boldsymbol{G} \in \Re^{k \times m_g}$ consists of external variables and $\boldsymbol{H} \in \Re^{k \times m_h}$ consists of main variables. The data matrix $\boldsymbol{H}$ of main variables should be decomposed into two parts: a part explained by the data matrix $\boldsymbol{G}$ of external variables and the other part not explained. For this purpose, multiple linear regression analysis can be used by regarding external variables and main variables as inputs and outputs, respectively. That is, a regression coefficient matrix $\boldsymbol{C} \in \Re^{m_g \times m_h}$ is determined so that the sum of squared errors or the squared Frobenius norm of an error matrix is minimized.

$$\boldsymbol{C} = (\boldsymbol{G}^T \boldsymbol{G})^{-1} \boldsymbol{G}^T \boldsymbol{H} \tag{2}$$

where the error matrix $\boldsymbol{E} \in \Re^{k \times m_h}$ is defined as

$$\boldsymbol{E} = \boldsymbol{H} - \boldsymbol{G}\boldsymbol{C}. \tag{3}$$

As a result, the main data matrix $\boldsymbol{H}$ can be decomposed into two parts, $\boldsymbol{G}\boldsymbol{C}$ and $\boldsymbol{E}$. $\boldsymbol{G}\boldsymbol{C}$ is a part explained by the external variables, and $\boldsymbol{E}$ is the other part that cannot be explained by the external variables. Any SPC method can be used for monitoring error variables. Equation (2) can be used only if external variables are linearly independent of each other. When external variables are highly correlated to each other, a multivariate data analysis technique such as PLS, which can cope with a collinearity problem, should be used instead of ordinary least squares.

When process dynamics cannot be ignored, the influence of changes in external variables cannot

be removed from operation data by using the static external analysis. In such a case, a dynamic model must be built. Kano et al. (2003) have proposed dynamic external analysis, and they have shown that the dynamic external analysis can be successfully applied to a chemical process.

2.2 *MSPC Integrated with External Analysis*

The basic statistic to monitor $\boldsymbol{E}$ in Eq. (3) is the Hotelling T^2 statistic. The Hotelling T^2 control chart is an original Shewhart-type control chart for correlated variables, and it is related to PCA-based SPC. PCA-based SPC was further investigated and a residual analysis was developed (Jackson and Mudholkar, 1979). In recent years, the T^2 statistic of several important principal components and the Q statistic, which is the sum of squared residuals or the sum of prediction errors (SPE), are usually used for statistical process monitoring. The T^2 statistic of principal components is defined as

$$T^2 = \sum_{r=1}^{R} \frac{t_r^2}{\sigma_{t_r}^2} \tag{4}$$

where t_r is a score of the r-th principal component and $\sigma_{t_r}^2$ is its variance. R denotes the number of principal components retained in the PCA model. The score t_r is defined as

$$\left[t_1 \ t_2 \ \cdots \ t_R \right] = \boldsymbol{eP} \tag{5}$$

where $\boldsymbol{e} \in \Re^{1 \times m_h}$ is an error vector, which is a row of $\boldsymbol{E}$, and $\boldsymbol{P} \in \Re^{m_h \times R}$ is a loading matrix. On the other hand, the Q statistic is defined as

$$Q = \sum_{i=1}^{m_h} (e_i - \hat{e}_i)^2 \tag{6}$$

where e_i and $\hat{e}_i$ are a calculated value of the i-th error variable and its predicted (reconstructed) value, respectively. $\hat{e}_i$ is derived from

$$\left[\hat{e}_1 \ \hat{e}_2 \ \cdots \ \hat{e}_{m_h} \right] = \boldsymbol{eP}\boldsymbol{P}^T \tag{7}$$

The T^2 statistic is a measure of the variation within the PCA model, and the Q statistic is a measure of the amount of variation not captured by the PCA model.

3. MONITORING A MONOMER PLANT

This section introduces an application of MSPC integrated with external analysis to a monomer plant of Mitsubishi Chemical Corporation. The main objective of this collaborative research project is to develop a monitoring system that can detect a particular malfunction as early as possible. The malfunction to detect is a blockage in an equipment of the monomer plant. Since the blockage, caused by an accumulation of polymers, requires shutdown maintenance, it is crucial to detect its symptom as early as possible and properly adjust the operating condition to prevent polymers from further accumulating. Conventional MSPC does not function well because it cannot distinguish the blockage from normal changes in operating conditions such as load changes. In the present work, therefore, external analysis is used to remove the influence of operating condition changes from process variables, and the error is monitored by using PCA-based SPC.

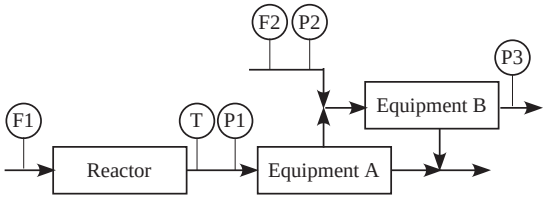

Fig. 1. Simplified PFD of the monomer plant.

Table 1. Process variables.

Symbol in Fig.1	Variable
F1	Raw material feed flow rate
F2	Recovery feed flow rate
P1	Equipment A inlet pressure
P2	Equipment A outlet pressure
P3	Equipment B outlet pressure
T	Reactor outlet temperature

3.1 *Malfunction in the Monomer Plant*

The process flow of the monomer plant is shown in Fig. 1. The product monomers are produced in the reactor, and then the reactant is condensed in the equipment A. Undesirable polymerization reactions take place under specific conditions in the equipment A although the operating condition is controlled to prevent monomers from polymerizing. The accumulation of polymers inside the equipment A blocks the flow and makes stable operation impossible.

Several important process variables are listed in Table 1. The symptom of the blockage could be detected by monitoring changes in differential pressure, P1-P2, because the blockage affects the pressure drop in the equipment A. The differential pressure will increase as more polymers accumulate. This monitoring strategy based on the differential pressure is very simple and easy to understand, but it is useful only when the differential pressure is not affected by other factors. In practice, not only polymer accumulation but also flow rates affect the

differential pressure. For efficient monitoring, it is necessary to take into account the influence of operating conditions on the differential pressure.

3.2 *Analysis of Abnormal Conditions*

Trend graphs of the measured process variables listed in Table 1 are shown in Fig. 2. The sampling period of each variable is one hour, and each graph includes 7500 samples (about 10 months). All six variables, except the differential pressure, P1-P2, are mean-centered.

The trend of P1-P2 shows that the differential pressure began to increase around 2000 hours. The uptrend of the differential pressure indicates the possibility of the polymer accumulation in the equipment A. Finally, at 2300 hours, operators gave up carrying on the operation and shut down the monomer plant. The blockage caused by polymer accumulation was found inside the equipment A. The monomer plant was restarted at 2800 hours after a considerable part of accumulated polymers were removed. However, further polymer accumulation proceeded after 3500 hours, and then the plant was shut down again. The plant was restarted at 4500 hours after the whole accumulated polymers were removed. The differential pressure increased again after the second start-up. In particular, the differential pressure after 6500 hours is higher than that in the period when polymers blocked the flow (2000-2300 hours). However, polymers did not accumulate and a blockage did not occur in that period. This fact indicates that a rise in the differential pressure does not necessarily mean a blockage and the differential pressure is affected by other factors. After 6500 hours, the recovery feed flow rate F2 decreased and consequently the pressures P1, P2, and P3 decreased. This change caused the differential pressure to increase. In addition, a load change also affects the differential pressure. The pressure measurements P1, P2, and P3 increased from 4500 to 6000 hours as the feed flow rate F1 increased. In this period, the differential pressure P1-P2 increased because of high throughput.

3.3 *Design of Monitoring System*

A rise in the differential pressure is a useful indicator for detecting the blockage, but it is also affected by operating conditions such as a feed flow rate. Therefore, the influence of operating conditions has to be removed from the differential pressure. For this purpose, the static external analysis was used. In this application, only static properties of the process should be taken into account because the sampling period is one hour.

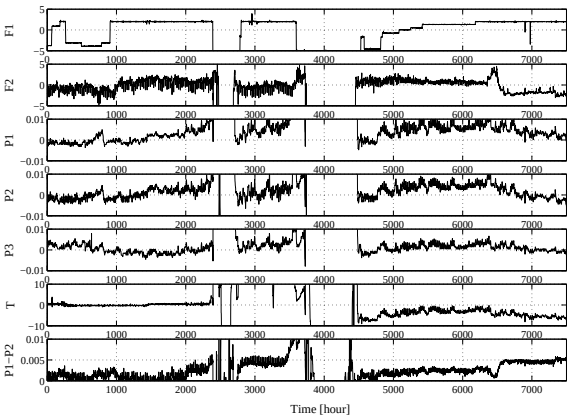

Fig. 2. Time-series plot of process variables.

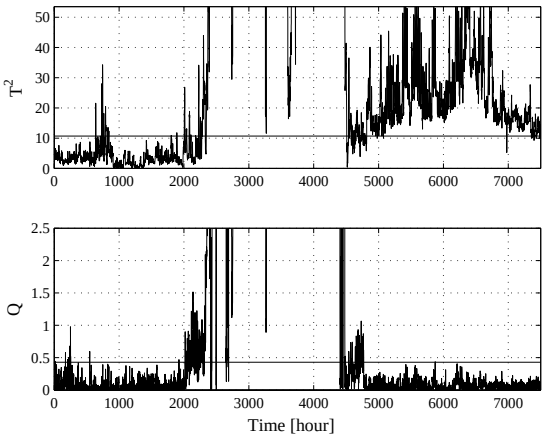

Fig. 3. Time-series plot of the T^2 and Q statistics.

The variables listed in Table 1 were used for monitoring. The external variables are the raw material feed flow rate F1 and the recovery feed flow rate F2. Those variables represent operating conditions. The other four variables were used as main variables.

External analysis and PCA were applied to data in the period when the process is operated under the normal condition (0-2000 hours), and the developed model was validated by the other data (2001-7500 hours except two shutdown periods). The number of principal components was selected so that the Q statistic could increase markedly when polymers accumulated. The selected number of principal components was three, and 98% of the variance in the reference data can be explained by three principal components. The control limits of two statistics are determined so that the number of samples outside the control limit is 1% of the entire samples while the process is operated under a normal condition. The control limits of T^2 and Q are 10.7 and 0.43, respectively.

3.4 *Monitoring Results*

The monitoring results, the trend graphs of T^2 and Q, are shown in Fig. 3. Although the

T^2 statistic exceeds its control limit from 2300 through 4500 hours, it also exceeds its control limit after 4500 hours. Therefore, the T^2 statistic is not a suitable index for detecting polymer accumulation. This result is not surprising because the T^2 statistic is a measure of the variation within the PCA model. The T^2 statistic is mainly affected by operating condition changes, which do not affect the correlation structure. As shown in Fig. 2, the operating condition of the monomer plant before 2000 hours is considerably different from that after 4500 hours. For example, the reactor outlet temperature is almost constant before 2000 hours, but it becomes lower and fluctuates wildly after 4500 hours. Such changes make the T^2 statistic exceed its control limit even though any fault does not occur. Since changes in the reactor outlet temperature cannot be explained by the external variables F1 and F2, the changes affect the T^2 statistic even when external analysis is conducted.

On the other hand, the Q statistic remarkably increases after 2000 hours and exceeds its control limit. The Q statistic is about 50 from 2800 to 3800 hours when polymers are blocking the flow. In addition, the Q statistic is under its control limit after accumulated polymers are removed. The Q statistic after 4800 hours is similar to that of the reference data even though the operating conditions are quite different from each other and the differential pressure increases considerably in this period. This result demonstrates the usefulness of the Q statistic for detecting polymer accumulation. It should be noted here, however, that conventional PCA-based SPC does not function well in this application. It cannot distinguish between polymer accumulation and operating condition changes. The key to success is to remove the influence of operating condition changes from monitored variables by conducting the external analysis.

Figure 3 shows that the Q statistic is a suitable index for detecting polymer accumulation. However, it is necessary to confirm that polymer accumulation is the real cause of the abnormal condition because another factor may affect the Q statistic and make it exceed the control limit. To identify the variables that contribute significantly to an out-of-control value of the Q statistic, contributions from process variables to the Q statistic can be used (Nomikos, 1996). This information helps operators to further diagnose an actual cause of the fault. A contribution of the i-th variable to the Q statistic is defined as

$$C_i = e_i - \hat{e}_i. \tag{8}$$

Contributions from four main variables to the Q statistic at the 2350th step are shown in Fig. 4.

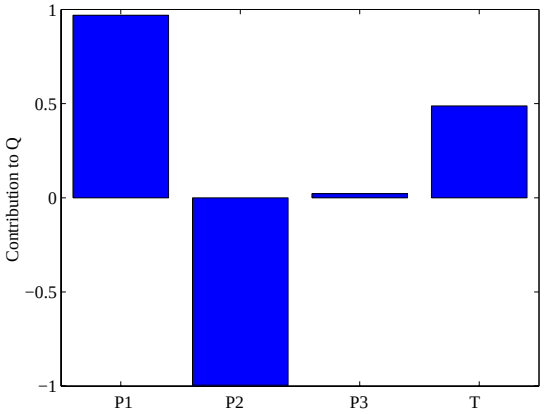

Fig. 4. Contribution plot of the Q statistic.

It is clear from this contribution plot that the contributions of the pressure of the equipment A, P1 and P2, are significant. P1 is positive large, and P2 is negative large. This result indicates that the differential pressure P1-P2 contributes significantly to the out-of-control value of the Q statistic. Therefore, polymer accumulation is the most possible cause. On the basis of this diagnosis, the operating condition should be adjusted to avoid a blockage caused by polymer accumulation.

3.5 *On-line Monitoring*

To monitor this monomer plant, in particular, to detect polymer accumulation, an on-line monitoring system was developed. The developed monitoring system performs the following procedures:

(1) Calculates the mean and the standard deviation of each monitored (external and main) variable, determines the regression coefficient matrix used for the external analysis, and builds the PCA model. This step is conducted off-line by using the reference data.
(2) Collects data every hour.
(3) Normalizes the data.
(4) Applies the external analysis to the normalized data.
(5) Calculates the Q statistic.
(6) Compares the calculated Q statistic and its control limit, and gives an alarm if Q exceeds its control limit.

The calculated Q statistic is stored in the database every hour, and its trend graph can be checked with trend graphs of monitored variables if necessary.

After the installation of the on-line monitoring system, polymer accumulation proceeded again in the equipment A. The external variables, F1 and F2, and the Q statistic are shown in Fig. 5. The recovery feed flow rate F2 was kept

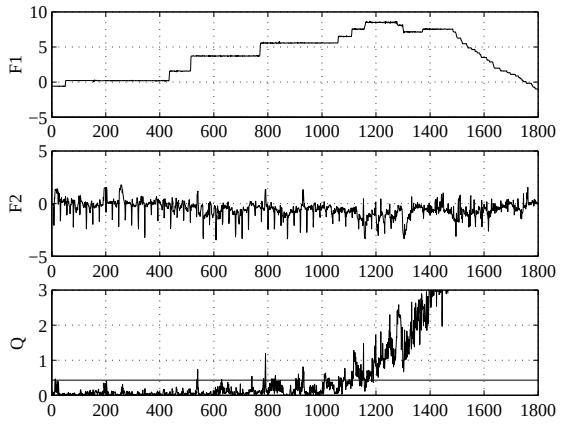

Fig. 5. On-line monitoring result.

almost constant during this period, but the raw material feed flow rate F1 was increased stepwise several times. The changes in the raw material feed flow rate did not affect the Q statistic, because the influence of the external variables was successfully removed from the monitored variables by using the external analysis. The Q statistic, however, increased steadily and exceeded its control limit after 1100 hours. This chart helped operators to suspect polymer accumulation and persuaded them to examine the equipment A. It was confirmed that polymer accumulation was proceeding. To avoid further accumulation of polymers and also to cope with the decrease in heat transfer efficiency, the raw material feed flow rate was decreased after 1280 hours. This result demonstrates that the developed on-line monitoring system, which integrates MSPC with external analysis, is useful for detecting polymer accumulation and avoiding a serious blockage in the monomer plant.

Another approach to avoid further polymer accumulation is to increase an inhibitor feed flow rate or a diluent water feed flow rate, which is used for cooling the reactant. Those approaches are useful, but they cannot remove the accumulated polymers. In the monomer plant, the equipment A consists of a number of parallel units. Therefore, the equipment A can be partially shut down and the accumulated polymers can be removed. As a result, by detecting polymer accumulation and avoiding a serious blockage, the developed monitoring system enables long-term, safe, and efficient operation of the monomer plant.

4. CONCLUSIONS

In this research project, PCA-based SPC was integrated with external analysis and applied to an industrial monomer plant. The developed monitoring system can distinguish polymer accumulation, which causes a serious blockage of the flow, from normal changes in operating conditions by using the static external analysis, and thus the system can successfully detect the polymer accumulation at its early stage. Although the developed monitoring system focuses only on the polymer accumulation in a particular equipment, it can detect symptoms of the most serious malfunction and persuade operators to take prompt and appropriate action. In practice, a reliable *specialist* is preferable to a moderate *generalist*. Various MSPC methods have been developed for general purposes in the last decade or so, but more important problems to investigate are how to diagnose the real cause of a serious fault and how to help operators to take appropriate action. Those problems seem to remain unsolved.

REFERENCES

Jackson, J.E. and G.S. Mudholkar (1979). Control Procedures for Residuals Associated with Principal Component Analysis. *Technometrics*, **21**, 341-349.

Kano, M., S. Hasebe, I. Hashimoto, and H. Ohno (2003). Evolution of Multivariate Statistical Process Control: Application of Independent Component Analysis and External Analysis. *Proc. of The Foundations of Computer Aided Process Operations Conference (FOCAPO)*, 358-388, Coral Springs, US, Jan. 12-15.

Kano, M., K. Miyazaki, S. Hasebe, and I. Hashimoto (2000). Inferential control system of distillation compositions using dynamic partial least squares regression. *J. Proc. Cont.*, **10**, 157-166.

Kano, M., K. Nagao, H. Ohno, S. Hasebe, I. Hashimoto, R. Strauss, and B.R. Bakshi (2002). Comparison of Multivariate Statistical Process Monitoring Methods with Applications to the Eastman Challenge Problem. *Comput. Chem. Engng*, **26**, 161-174.

Kourti, T. and J.F. MacGregor (1995). Process Analysis, Monitoring and Diagnosis, Using Multivariate Projection Methods. *Chemometrics and intelligent laboratory systems*, **28**, 3-21.

Kresta, J.V., J.F. MacGregor, and T.E. Marlin (1991). Multivariate Statistical Monitoring of Process Operating Performance. *Can. J. Chem. Eng.*, **69**, 35-47.

Ku, W., R.H. Storer, and C. Georgakis (1995). Disturbance Detection and Isolation by Dynamic Principal Component Analysis. *Chemometrics and intelligent laboratory systems*, **30**, 179-196.

Nomikos, P. (1996). Detection and diagnosis of abnormal batch operations based on multi-way principal component analysis. *ISA Trans.*, **35**, 259-266.

ON-LINE MONITORING OF A COPOLYMER REACTOR: A CASCADE ESTIMATION DESIGN

Teresa Lopez [(1)], Jesus Alvarez [(2)] and Roberto Baratti [(3)]

[(1)] *Instituto Mexicano del Petróleo, Programa de Matemáticas Aplicadas y Computación, Lazaro Cardenas 152, A.P. 14-805, 07730 Mexico D.F., Mexico (mtlopeza@imp.mx)*
[(2)] *Departamento de Ingenieria de Procesos e Hidraulica, Universidad Autonoma Metropolitana - Iztapalapa, 09340 Mexico D.F., Mexico (jac@xanum.uam.mx)*
[(3)] *Dipartimento di Ingegneria Chimica e Materiali, Universita' di Cagliari, Piazza D'Armi, 09123 Cagliari, Italy (baratti@dicm.unica.it)*

Abstract: In this work the problem of on-line monitoring of product quality and production rate in a copolymer reactor is addressed, using an estimation scheme with secondary measurements of density, refractive index, temperature, and volume. Three different estimator structures are studied: (a) the nominal detectability structure that underlines the extended Kalman filter and Luenberguer observers, (b) a passive estimation structure with estimation degrees equal to one, and (c) a hybrid structure that combines the detectability and passive structures in low and high gain, respectively. The nominal detector maximizes the reconstruction rate, the passive estimator maximizes the robustness, and the cascade (hybrid) design achieves a suitable compromise between them. The approach is illustrated with a copolymer reactor case and simulations.

Keywords: Chemical industry, Monitoring, Extended Kalman filter, Geometric approach, Observability, Detectors, State estimation.

1. INTRODUCTION

Copolymerization is an important industrial process where commodity and engineering plastics are manufactured. In a continuous reactor operation, the knowledge of the instantaneous copolymer properties (such as copolymer composition, conversion, mass fraction, molecular weight, etc.) is important for on-line monitoring, control, and fault detection purposes. These properties have direct implications in the safety, product quality and production rate performance indices, but they are not available on-line. Thus, the estimation objective is the inference of variables related to product quality and production rate using a model-based estimation technique with secondary on-line measurements (Mutha et al., 1997; Dimitratos et al., 1991; Ellis et al, 1994; Van Dooting et al., 1992).

In polymer reactor engineering, the Extended Kalman Filter (EKF) is the most widely used state estimation technique, and the Luenberguer observer (LO) has been increasingly considered in the last decade. In both techniques, their structure is fixed and determined by the nominal observability property. If this property is ill-conditioned, any appropriately constructed and tuned detector should diverge or malfunction. To tackle this problem, the idea of considering the estimator structure as a degree of freedom to improve its functioning was proposed in the geometric estimation design (Alvarez and Lopez, 1999; Alvarez, 2000). In Hernandez and Alvarez (2003), the corresponding definition of nonlinear estimability (a robust form of detectability) was put in formal perspective with the existing indistinguishability-based definitions of nonlinear detectability (Hermann and Krener, 1977; Sontag, 1990). In Alvarez and Lopez (2003), the effect of the estimator structure on its functioning was studied for a representative case study of a copolymer reactor, showing that: (i) the structure decision problem is not trivial in the sense that there are 56 possible estimator

structures for the case study; (ii) the best functioning is attained neither with the nominal detectability structure associated with the standard EKF and LO nor with a passive estimation structure (i.e. with estimation degrees equal to one), but with an intermediate structure; and (iii) how the estimation structure determines the estimator reconstruction rate and the error propagation mechanism.

Having as a point of departure the aforementioned results on the copolymer reactor case (Lopez and Alvarez, 2003), in this work the problem of on-line inferring the safety, quality and production rate is addressed. Using the geometric estimation approach with secondary measurements of density, refractive index, temperature, and volume. Considering that the nominal detector maximizes the innovated dynamics dimension and therefore the reconstruction rate, and that the passive estimator maximizes the robustness to modeling errors. Here the idea is to use a hybrid structure that superimposes a fast passive estimator with the slow nominal detector, obtaining a cascade estimator that yields a better compromise between reconstruction rate and robustness. The three estimator designs (nominal detector, passive estimator and cascade design) are illustrated with a copolymer reactor case and simulations.

2. THE COPOLYMER REACTOR PROBLEM

2.1 The reactor model

Let us consider a continuous reactor where a solution copolymerization takes place (see Fig. 1). The reactions are strongly exothermic, and heat is removed by means of a cooling jacket. There is significant gel-effect (i.e., reaction autoacceleration by diffusional limitations in the mobility of the copolymer chains), meaning a copolymer conversion accompanied by a considerable viscosity increase and a decrease in the heat exchange capability. From standard kinetics, reaction engineering, and viscous heat exchange modeling considerations, the reactor model is given as follows (functions and parameters defined in Padilla and Alvarez, 1996):

$$\dot{m}_1 = -r_1 + (q_1 m_{1e} - q_e m_1)/V := f_1(m_1,m_2,p_1,p_2,i,T,V)$$

$$\dot{m}_2 = -r_2 + (q_2 m_{2e} - q_e m_2)/V := f_2(m_1,m_2,p_1,p_2,i,T,V)$$

$$\dot{p}_1 = -r_1(1-\varepsilon_1) + (q_1 p_{1e} - q_e p_1)/V := f_3(m_1,m_2,p_1,p_2,i,T,V)$$

$$\dot{p}_2 = -r_2(1-\varepsilon_2) + (q_2 p_{2e} - q_e p_1)/V := f_4(m_1,m_2,p_1,p_2,i,T,V)$$

$$\dot{i} = -r_I + (w_I - q_e i)/V := f_5(i,T,V)$$

$$\dot{T} = r_T - \gamma(T-T_c) + q_{he} - q_h := f_6(m_1,m_2,p_1,p_2,i,T,V)$$

$$\dot{V} = q_e - q := f_7(m_1,m_2,p_1,p_2,i,T,V)$$

$$\dot{\mu}_0 = r_{\mu 0} + [(q_1+q_2)\mu_{0e} - q_e\mu_0)/V := f_8(m_1,m_2,p_1,p_2,i,T,V,\mu_0)$$

$$\dot{\mu}_2 = r_{\mu 2} + [(q_1+q_2)\mu_{2e} - q_e\mu_2)/V := f_9(m_1,m_2,p_1,p_2,i,T,V,\mu_2)$$

where

$$q_e = q_1\phi_1 + q_2\phi_2 + q_s\phi_s + (r_1\phi_4 + r_2\phi_5)V$$

$$q_h = (q_1\rho_1 + q_2\rho_2 + q_s\rho_s)T/(\rho V)$$

$$q_{he} = (q_1\rho_1 C_{p1} T_{1e} + q_2\rho_2 C_{p2} T_{2e} + q_s\rho_s C_{ps} T_{se})/(\rho V C_p)$$

The reactor states (x) are: the dimensionless concentrations (referred to pure materials) of the i-th monomer (m_i), of the i-th converted monomer (p_i), and of the initiator (i); the temperature (T), the volume (V), and the zeroth (μ_0) and second (μ_2) moments of the chain length distribution (CLD). The exogenous inputs (u) are: the feed concentration of i-th monomer (m_{ie}), and of the i-th converted monomer (p_{ie}); the feed temperatures of the i-th monomer (T_{ie}), and of the solvent (T_{se}); the jacket temperature (T_c), the feed flowrate of the i-th monomer (q_i), and of the solvent (q_s); the mass feedrate of initiator (w_{Ie}); and the exit flowrate (q). The total feed flowrate (q_e) is corrected by the contraction of volume due to the polymerization, where (ϕ_1, ϕ_2, ϕ_3, ϕ_4, ϕ_5) is equal to (1, 1, 1, 0, 0) if no volume contraction is considered. While the dimensionless solvent concentration (s) is given by

$$s = 1 - (m_1 + m_2 + p_1 + p_2)$$

The following set of scalar fields are smooth and strictly positive: the rates of initiator decomposition (r_I), polymerization of monomers 1 (r_1) and 2 (r_2), and change of the zeroth ($r_{\mu 0}$) and second ($r_{\mu 2}$) CLD moments, the ratios of heat generation (r_T) and exchange (γ) to heat capacity, the input (q_{he}) and the output (q_h) enthalpy flows. The measured outputs (y) are the density (ρ), the refractive index (η), the temperature (T), and the volume (V):

$$y_1 = \rho, \qquad y_2 = \eta, \qquad y_3 = T, \qquad y_4 = V$$

where ρ is calculated by volume additivity and η according the Lorimer theory (1972):

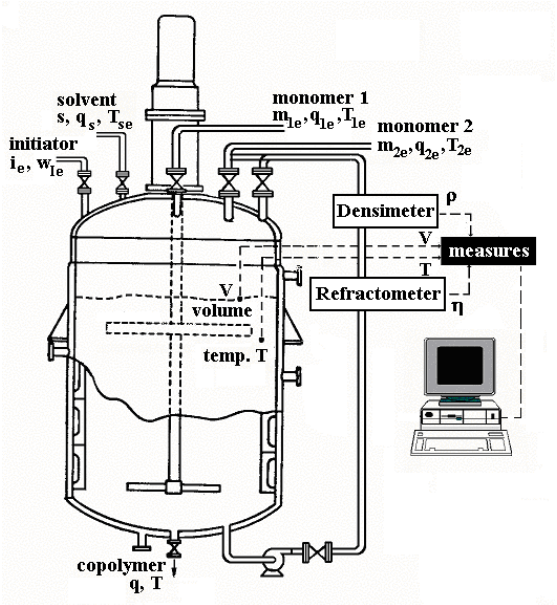

Fig. 1. The copolymerization reactor.

$\rho = m_1\rho_1^o + m_2\rho_2^o + p_1\rho_1^p + p_2\rho_2^p + s\rho_s^o := h_1(m_1,m_2,p_1,p_2)$

$\eta = \eta_o + C_s\nu + a_2C_s^2 := h_2(m_1,m_2,p_1,p_2)$

The outputs (z) to be inferred are: the instantaneous composition (z_c) of monomer 1, the conversion (z_p) of copolymer, the weight-average molecular weight (z_M) of the CLD, and the production rate (z_R) of copolymer:

$z_c = r_1M_1^o / (r_1M_1^o + r_2M_2^o) := g_1(m_1, m_2, p_1, p_2, i, T)$

$z_p = (p_1P_1^o + p_2P_2^o) / (m_1M_1^o + m_2M_2^o + p_1P_1^o + p_2P_2^o)$
$:= g_2(m_1, m_2, p_1, p_2)$

$z_M = \mu_2 / (p_1P_1^o + p_2P_2^o) := g_3(p_1, p_2, \mu_2)$

$z_R = (r_1\rho_1^o + r_2\rho_2^o)V := g_4(m_1, m_2, p_1, p_2, i, T)$

which are key variables to monitor the product quality and the production rate.

In compact notation, the reactor model can be as follows:

$$\dot{x} = f(x, u, p), \qquad y = h(x, p), \qquad z = \eta(x, p) \qquad (1)$$

where p is the vector of model parameters, and

$x = [m_1, m_2, p_1, p_2, i, T, V, \mu_0, \mu_2]^T$

$y = [y_\rho, y_\eta, y_T, y_T]^T$

$u = [m_{1e},m_{2e},p_{1e},p_{2e},T_{1e},T_{2e},T_{se},T_c,q_1,q_2,q_s,w_{Ie},q]^T$

$z = [z_c, z_p, z_M, z_R]^T$

2.2 Reactor dynamics

As a case study, the copolymerization of methyl methacrylate (MMA) and vinyl acetate (VAC) is considered, with ethyl acetate (AE) as solvent and azo-bis-isobutyronitrile (AIBN) as initiator. In steady-state operation, the copolymer reactor may exhibit multiplicity of critical points (Hamer *et al*., 1981). The nominal input

$u = [1.0, 1.0, 0.0, 0.0, 315\ K, 315\ K, 315\ K, 328\ K,$
$1.11x10^{-3}\ m^3/min, 6.23x10^{-3}\ m^3/min, 1.99x10^{-3}$
$m^3/min, 6.66x10^{-5}\ Kmol/min, 8.53x10^{-3}\ m^3/min]^T$

was chosen such that the reactor had three steady-states: two of them (ignition and extinction-type) are stable, and one is unstable. To test the functioning of the proposed estimation designs, the following reaction motion was considered. Initially, the reactor is at its unstable steady-state, and the four exogenous inputs $u(t) = [m_{1e}(t), T_{1e}(t), T_{2e}(t), T_{se}(t)]^T$ are varied as shown in Fig. 2. As a result, the reactor is driven to its ignition-type steady-state after undergoing a transient with ample and abrupt changes in its state, as it can be seen in the continuous thick curves of Fig. 4. This drastic motion must be regarded as the extreme case of a practical situation, in order to subject the proposed estimation scheme to a severe test.

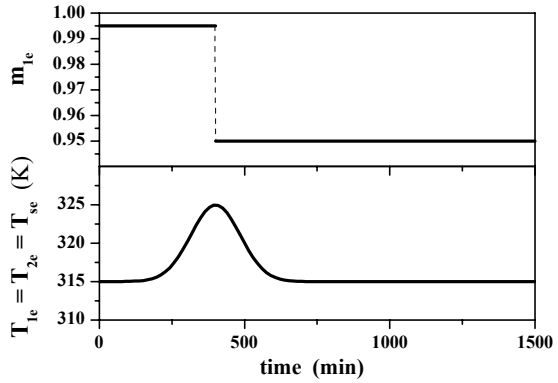

Fig. 2. Time-varying exogenous inputs.

2.3 The on-line monitoring problem

Our main objective is the on-line inference of the variables (z) related to product quality (instantaneous composition, conversion and molecular weight) and production rate, using a robust estimation design with on-line secondary measurements (y) of density, refractive index, temperature, and volume.

As mentioned before, this reactor admits 56 estimator structures (Lopez, 2000; Alvarez and Lopez, 2003), including the nominal detectability structure associated to the standard EKF and LO designs. However the best functioning is attained nor with the nominal detectability structure either with a passive structure, but with an intermediate one. Here, a constructive-like framework (Sepulchre *et al*., 1997) is recalled to design a cascade estimator to improve its behavior: a low gain detectability structure is cascaded to a high gain passive structure in order to obtain a better compromise between reconstruction rate and robustness to modeling errors.

3. NONLINEAR ESTIMATION

In this section, the notions of nominal and robust nonlinear detectability are defined according Alvarez and Lopez (1999) and Hernandez and Alvarez (2003). The construction of the geometric high-gain observer follows from a straightforward consequence of the detectability property. The estimator construction, the convergence criterion, and the tuning technique can be found in Alvarez and Lopez (1999) and Alvarez (2000). Then, the nominal and passive structures of the copolymer reactor case are recalled (Lopez, 2000; Lopez and Alvarez, 2003). Then, the cascade structure is introduced and justified. Finally, three estimator designs are presented and compared: the nominal detector, the passive estimator and the cascade design.

3.1 Detectable and passive structures

From Lopez (2000) and Lopez and Alvarez (2003), we know that the copolymer reactor [Eq. (1)] motion is nominally detectable (i.e. the observability matrix

has maximum rank) with the structure:

$$S_D = (\underline{k}, x_o, x_\mu) \quad (2)$$

where $\underline{k}$ is the observability index vector, and x_o (or x_μ) is the observable (or unobservable) state:

$$\underline{k} = (k_1, k_2, k_3, k_4) = (2, 2, 2, 1), \quad k = \sum k_i = 7 \quad (3a)$$

$$x_o = [x_1, \ldots, x_7]^T = [m_1, m_2, p_1, p_2, i, T, V]^T \quad (3b)$$

$$x_\mu = [x_8, x_9]^T = [\mu_0, \mu_2]^T \quad (3c)$$

This detectability property with partial observability follows from the fulfillment of two conditions: (i) the observability matrix O has rank 7 over time, and (ii) the unobservable motion x_μ (t) is stable. This is,

$$\text{Rank } O(x, u, p, \underline{k}) = 7 \quad \forall\, t \quad (4a)$$

$$O(x, u, p, \underline{k}) = \partial\phi/\partial x_o, \qquad \dim O = k = 7 \quad (4b)$$

$$\phi(x, u, p, \underline{k}) = [h_1, (\partial h_1/\partial x)\, f, h_2, (\partial h_2/\partial x)\, f, x_6, f_6, x_7]^T$$

and the unobservable dynamics

$$\dot{x}^*_\mu = [f_8, f_9]^T[\phi^{-1}(u, p, \underline{k}), x^*_\mu, u, p] := f_\mu(x_o, x^*_\mu, u, p) \quad (5a)$$

have a (unique) stable solution

$$x^*_\mu(t) = \theta_\mu(t, t_0, x^*_{\mu 0}, u, p, \underline{k}) \quad (5b)$$

The nominal detectability structure S_D [Eq. (2)] is the one that, over the set of 56 admissible structures, maximizes the dimension of the innovated (i.e., with measurement injection) dynamics, or equivalently, the reconstruction rate, regardless of robustness considerations. If the observability matrix [Eq. (4b)] is ill-conditioned, any nominal detectability-based observer should malfunction or diverge.

In the spirit of the passivation backstepping procedure (Sepulchre *et al*., 1997; Kristic *et al*., 1995), let us recall the passive structure (Lopez and Alvarez, 2003)

$$S_P = (\underline{\kappa}, x_I, x_{II}) \quad (6)$$

that maximizes the robustness at the cost of the reconstruction rate. $\underline{\kappa}$ is the estimation degree vector, and x_I (or x_{II}) is the innovated (or non-innovated) state:

$$\underline{\kappa} = (\kappa_1, \kappa_2, \kappa_3, \kappa_4) = (1, 1, 1, 1), \quad \kappa = \sum \kappa_i = 4 \quad (7a)$$

$$x_I = [x_1, x_2, x_6, x_7]^T = [m_1, m_2, T, V]^T \quad (7b)$$

$$x_{II} = [x_3, x_4, x_5, x_8, x_9]^T = [p_1, p_2, i, \mu_0, \mu_2]^T \quad (7c)$$

This estimability property (with minimum innovation) follows from the fulfillment of two conditions: (i) the innovation matrix O has rank 4 over time, and (ii) the non-innovated motion $x_{II}(t)$ is stable. This is,

$$\text{Rank } O(x, u, p, \underline{\kappa}) = 4 \quad \forall\, t \quad (8a)$$

$$O(x, u, p, \underline{\kappa}) = \partial\phi/\partial x_I, \qquad \dim O = \kappa = 4 \quad (8b)$$

$$\phi(x, u, p, \underline{\kappa}) = [h_1, h_2, x_6, x_7]^T$$

and the non-innovated dynamics

$$\dot{x}^*_{II} = [f_3, f_4, f_5, f_8, f_9]^T[\phi^{-1}(u, p, \underline{\kappa}), x^*_{II}, u, p] := f_{II}(x_I, x^*_{II}, u, p) \quad (9a)$$

have a (unique) stable solution

$$x^*_{II}(t) = \theta_{II}(t, t_0, x^*_{II0}, u, p, \underline{\kappa}) \quad (9b)$$

Figure 3 shows the condition number of the observability (or innovation) matrix [Eqs. (4b) or (8b)] associated to the nominal detectability (or passive) structure S_D (or S_P), showing that the observability matrix is significantly more ill-conditioned (by 5 order of magnitude) than the passive innovation matrix.

3.3 Cascade structure

In the adjustable structure estimation study presented in Lopez and Alvarez (2003), it was established that the best estimator behavior was attained with an intermediate degree (k = 5) structure, and not with the detectability (k = 7) or passive (κ = 4) structure. In the understanding that the detectability structure is the one that underlies the well known nonlinear EKF and LO. Motivated by the structure-oriented nonlinear constructive control approach (Sepulchre *et al*., 1997; Kristic *et al*., 1995), in the present work a different way to obtain a better estimator behavior is considered: the cascade combination of a low gain detectability structure with a high gain passive structure. According to the following rationale: (i) first, a high-gain passive estimator (i.e, with fast dynamics) is designed in order to quickly and robustly match the input-output reactor behavior, regarding this estimator as a redesigned model, and then (ii) a low-gain nominal detector is designed for this new model, in order to reconstruct the maximum number of states. This idea has been applied successfully in a catalytic reactor with experimental data (Lopez *et al.*, 2002). However in this catalytic reactor the structure estimation choice was not a complex task because there are only two candidate structures. While in our copolymer reactor case there are 56 admissible estimation structures.

To define the cascade structure, let us consider the following state partition:

$$x = [x_I, x_P, x_\mu]^T \quad (10a)$$

$$x_I = [x_1, x_2, x_6, x_7]^T = [m_1, m_2, T, V]^T \quad (10b)$$

$$x_P = [x_3, x_4, x_5]^T = [p_1, p_2, i]^T \quad (10c)$$

$$x_\mu = [x_8, x_9]^T = [\mu_0, \mu_2]^T \quad (10d)$$

where x_P is made by the observable states [Eq. (3b)] transferred from the observable state (x_o) to the non-innovated one (x_{II}).

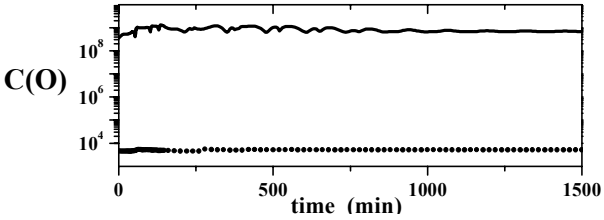

Fig. 3. Condition number C(O) of the observability (———) or innovation (·····) matrices [Eqs. (4b) or (8b)] associated to the detectability (S_D) and passive (S_P) structures.

3.4 Estimators

Nominal detector. The PI (proportional - integral) estimator construction follows from a straightforward application of Theorem 2 given in Alvarez and Lopez (1999), obtaining the following nominal detector:

$$\dot{\hat{x}}_o = f_o(\hat{x}, u, \hat{p}) + G(\hat{x}, u, \hat{p}, \underline{k}, s)\,[y - h(\hat{x}, \hat{p})] + H(\hat{x}, u, \hat{p}, \underline{k}) \int K_I(\underline{k}, s)\,[y - h(\hat{x}, \hat{p})]dt \quad (11a)$$

$$\dot{\hat{x}}_\mu = f_\mu(\hat{x}, u, \hat{p}) \quad (11b)$$

$$\hat{y} = h(\hat{x}, \hat{p}), \quad \hat{z} = g(\hat{x}, \hat{p}), \quad \hat{x} = [\hat{x}_o, \hat{x}_\mu]^T \quad (11c)$$

Here the nonlinear gains are given by

$$[G, H](\hat{x}, u, \hat{p}, \underline{k}, s) = O^{-1}(\hat{x}, u, \hat{p}, \underline{k})\,[K_p(\underline{k}, s), \Pi(k)]$$

O^{-1} is the inverse of the observability matrix, and $\{\Pi, K_P, K_I\}$ are given by (bd := block diagonal)

$$\Pi(k) = bd[\pi_1, \pi_2, \pi_3, \pi_4], \qquad \dim \Pi = k \times 4$$

$$K_P(k, s) = bd[k_{p1}, k_{p2}, k_{p3}, k_{p4}], \quad \dim K_P = k \times 4$$

$$K_I(k, s) = diag[(s\omega_1)^{k_1+1}, (s\omega_2)^{k_2+1}, (s\omega_3)^{k_3+1}, (s\omega_4)^{k_4+1}]$$

$$\pi_i = [1], \qquad k_{pi} = [s\omega_i] \quad \text{if } k_i = 1$$

$$\pi_i = [0, 1]^T, \quad k_{pi} = [(2\zeta+1)s\omega_i, (2\zeta+1)(s\omega_i)^2]^T \quad \text{if } k_i = 2$$

where (ω_i, ζ, s) are the output reference frequencies (one for each measurement), the reference damping factor, and the celerity estimator parameter, which are considered as tuning parameters.

Passive estimator. In this case the design is equivalent to previous estimator [Eqs. (11)] but replacing the observability index vector $\underline{k}$ [Eq. (3a)] by $\underline{\kappa}$ [Eq. (7a)], the observability matrix O [Eq. (4b)] by the innovation one [Eq. (8b)], the state partition [Eqs. (3b) and (3c)] by [Eqs. (7b) and (7c)], and the unobservable dynamics [Eq. (5a)] by the non-innovated dynamics [Eq. (9a)].

Cascade design. The application of the construction guidelines given in the previous subsection yields the cascade estimator:

$$\dot{\hat{x}}_I = f_I(\hat{x},u,\hat{p}) + \big[G(\hat{x},u,\hat{p},\underline{\kappa},s_f) + G(\hat{x},u,\hat{p},\underline{k},s_s)\big][y-h(\hat{x},\hat{p})] + \big[H(\hat{x},u,\hat{p},\underline{\kappa})K_I(\underline{\kappa},s_f) + H(\hat{x},u,\hat{p},\underline{k})K_I(\underline{k},s_s)\big] \int [y - h(\hat{x},\hat{p})]dt \quad (12a)$$

$$\dot{\hat{x}}_P = f_P(\hat{x},u,\hat{p}) + G(\hat{x},u,\hat{p},\underline{k},s_s)\,[y - h(\hat{x},\hat{p})] + H(\hat{x},u,\hat{p},\underline{k})\,K_I(\underline{k},s_s) \int [y - h(\hat{x},\hat{p})]dt \quad (12b)$$

$$\dot{\hat{x}}_\mu = f_\mu(\hat{x},u,\hat{p}) \quad (12c)$$

$$\hat{y} = h(\hat{x},\hat{p}), \quad \hat{z} = g(\hat{x},\hat{p}), \quad \hat{x} = [\hat{x}_I, \hat{x}_P, \hat{x}_\mu]^T \quad (12d)$$

where s_s (or s_f) is the slow (or fast) celerity parameter that sets the convergence rate of the associated passive estimator (or detector). In this way, the convergence rate of x_I (or x_P) is affected by (s_s, s_f) (or s_s), and the convergence rate of the non-innovated state x_μ is independent of (s_s, s_f).

The convergence conditions for the detector and passive estimators [Eqs. (11)] are given in Alvarez and Lopez (1999). The technical derivation of the convergence criterion of the proposed cascade design [Eqs. (12)] goes beyond the scope of the present work. Here, it suffices to say that the application of the singular perturbation arguments employed in standard cascade control design yields that the proposed cascade estimator is convergent if: (i) first, with the slow parameter defined ($s_s = 0$), the parameter s_f is tuned sufficiently fast (typically 3 to 15 times the reactor natural dynamics) so that the passive estimator robustly converges, and (ii) then, the parameter s_s is chosen sufficiently slow ($s_s > 0$) so that the cascade estimator functions with an adequate trade off between reconstruction rate and robustness.

4. ESTIMATOR IMPLEMENTATIONS

4.1 Tuning

The nominal detector and the passive estimator were tuned following the pole-placement geometric estimation tuning scheme presented in Alvarez and Lopez (1999). The output reference frequencies were set as $(\omega_1,\omega_2, \omega_3, \omega_4) = (1/2, 1/2, 2, 2)\omega_r$, where $\omega_r = 1/\tau_r$ min^{-1} is the characteristic time of the average reactor residence time τ_r = 200 min. The damping factor was set as $\zeta = 0.71$, and the celerity parameter was set at $s = 10$ for both designs, meaning that their dynamics are set ten times faster than the natural output dynamics.

Following the tuning guidelines presented in the last subsection, the cascade estimator was tuned as follows: (i) the value $s_f = 10$ of the passive estimator was adopted, (ii) the damping factor $\zeta = 0.71$ was fixed, and (iii) the parameter s_s was gradually increased until a satisfactory functioning was attained at $s_s = 4$.

4.2 Functioning

To evaluate the estimator functioning, the estimator model was run with the following errors: -4% error in the activation energies of propagation, -20% error in the heat transfer coefficient, and no volume contraction (i.e., $\phi_1 = \phi_2 = \phi_3 = 1$ and $\phi_4 = \phi_5 = 0$).

The detector and passive estimator estimates are shown in Fig. 4. The detector estimates (thin continuous plots) exhibit a fast oscillation response with some offset. The passive estimator (discontinuous plots) has a behavior in the other way around: slow non-oscillatory convergence with larger offset. These results (Lopez and Alvarez, 2003) are in agreement with the conditioning assessment of the observability and passive innovation matrices presented in Fig. 3.

The cascade estimator functioning presented in Fig. 4, showing the estimates, has effectively achieved a

better compromise between performance and robustness: the behavior retains features of both nominal and passive structures, so the motions are slightly oscillating (mainly for the composition), there are minor offsets, and fast convergence rates are attained.

7.CONCLUSIONS

The problem of the product quality and production rate inference has been addressed of a copolymer reactor, using on-line secondary measurements. Three different nonlinear estimation structures were considered: (a) the nominal detectability structure, that maximizes the reconstruction rate, (b) the passive estimation structure that maximizes the robustness, and (c) the proposed cascade estimation structure which superimposes a fast passive detector with a slow nominal detector, achieving a better compromise between performance (fast reconstruction rate) and robustness (tolerance to modeling error and error propagation). Invoking singular perturbation arguments, the cascade estimator convergence was established in terms of a cascade control like criterion: a fast passive gain with a sufficiently slow detectability gain.

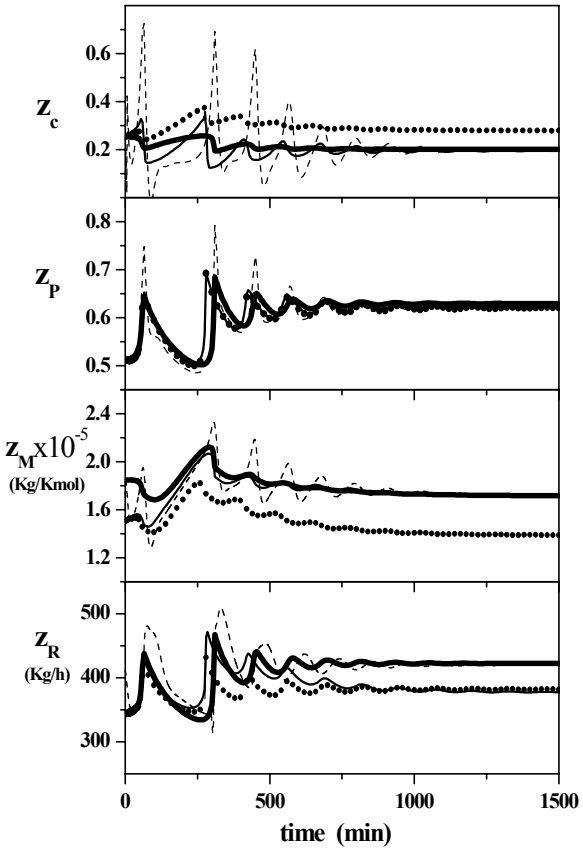

Fig. 4. Dynamic response of the reactor (——), of the detector (– – –), of the passive estimator (.....), and of the cascade estimator (———).

REFERENCES

Alvarez, J. (2000). Nonlinear state estimation with robust convergence, *J. Proc. Control*, 10, 59.

Alvarez, J. and T. López (1999). Robust Dynamic State Estimation of Nonlinear Plants, *AIChE J.*, 45(1), 107.

Dimitratos, J., C. Georgakis, M. El-Aasser and A. Klein (1991). An Experimental Study of Adaptive Kalman Filtering in Emulsion Copolymerization. *Chem. Eng. Sci*., 46, 3203-3218.

Ellis, M.F., T.W. Taylor and K.F. Jensen (1994). On-line Molecular Weight Distribution Estimation and Control in Batch Polymerization Reactors. *AIChE J.*, 40, 445-462.

Hamer, J.W., T.A. Akramov and W.H. Ray (1981). The Dynamic Behavior of Continuos Polymerization Reactors - II. Nonisothermal Solution Homopolymer. and Copolymerization in a CSTR. *Chem. Eng. Sci.*, 36, 1897-1914.

Hermann, R. and A.J. Krener (1997). Nonlinear controllability and observability, *IEEE TAC AC*-22, 5.

Hernandez, H. and J. Alvarez (2003). Robust estimation of continuous nonlinear plants with discrete measurements, *J. Proc. Control*,13(1), 69

Lopez, T. (2000). Estimacion y control no lineal de reactores de copolimerizacion. *Ph. D. Thesis*, Universidad Autonoma Metropolitana, Mexico.

Lopez, T. and J. Alvarez (2003). On the effect of the estimation structure in the functioning of a nonlinear copolymer reactor estimator, submitted to the *J. Proc. Control*.

Lopez, T., S. Tronci, R. Baratti, and J. Alvarez (2002). State estimation in a catalytic reactor via a constructive approach, *Proc. IFAC World Cong*., Barcelona, Spain.

Lorimer, J.W. (1972). Refractive index increments of polymers in solution: 3. Dependence on concentration, *Polymer*, 13, 274.

Mutha, R. K., W.R. Cluett, and A. Penlidis (1997). On-line nonlinear model-based estimation and control of a polymer reactor, *AIChE J*., 43, 3042.

Kristic, M., I. Kanellapoulos and P. Kokotovic (1995). *Nonlinear and Adaptive Control Design*. Wiley, New York.

Padilla, S. and J. Alvarez (1997). Control of Continuous Solution Copolymerization Reactors. *AIChE J*., 43(2), 448.

Ray, W.H. (1986). Polymerization Reactor Control, *IEEE Control systems,* 6(4), 3.

Sepulchre, R., Jankovic, M. and Kokotovic, P.V. (1997). *Constructive Nonlinear Control*. Springer-Verlag, London

Sontag, E. D. (1990). *Mathematical control theory, Deterministic finite dimensional systems*. Springer-Verlag, New York.

Van Dooting, M., V.D. Rakotrapa, J.P. Gauthier and P. Hobbes (1992). Nonlinear Deterministic Observer for State *Estimation*: Application to a Continuous Free-Radical Polymerization Reactor, *Comp. Chem. Eng*. 16, 777.

A ROBUST PCA MODELING METHOD FOR PROCESS MONITORING

D. Wang and J.A. Romagnoli

Dept. of Chemical Engineering,
The University of Sydney, NSW 2006 Australia

Abstract: A robust method for dealing with the gross errors in the data collected for PCA model is proposed. This method, using M-estimator based on the generalized t distribution, adaptively transforms the data in the score space in order to eliminate the effects of the outliers in the original data. The robust estimation of the covariance or correlation matrix is obtained by the proposed approach so that the accurate PCA model can be obtained for the process monitoring purpose. Comparisons with the conventional PCA modeling and other robust outlier's replacement approaches are illustrated through a chemical engineering example.

Keyword: Principal component analysis, multivariate outliers, robust estimation, winsorization, process monitoring.

1 INTRODUCTION

Data-driven process monitoring based on multivariate statistic techniques is widely used in chemical industries with a large amount of measurements provided by the modern hardware. The measurement variables are usually highly correlated and the real dimensionality of the process variables is considerably less than that represented by the number of process variables collected. Monitoring this "data rich" process inevitably need dimensionality reduction techniques to grasp the driven force embedded in these measurements. By converting the large amount of data collected from the process into a few meaningful measures, one can assist the industrial operators in determining the status of the operations and in detecting and diagnosing the faults. Principal components analysis (PCA) is such a dimensionality reduction technique and it is heavily used in modeling the multivariate process for monitoring purpose (Kresta, et. al., 1991).

The performance of PCA model is based on the accurate estimation of the covariance or correlation structure of the data. The optimality of the conventional PCA is based on the assumption that the data are normal distributed around their locations with the scales. However, normal distribution usually dose not exist in real chemical engineering practice, it is hard to assure the normality even for high quality measurements. Specially, the frequent presence of gross errors and outliers violates the assumptions in the conventional approach (even through the data is auto scaled) and makes the results invalid (Hoo, K. A. et. al., 2002).

Several approaches can be employed to alleviate the outlier problem in PCA modeling. One of them is based on filter approaches to detect the gross outliers and delete them or replace them with some values before the conventional PCA is used. This pre-treatment approach is intuitive but it may suffer information and performance loss due to its subjective or ad hoc fashion. In addition, the multiple outliers are hard to be detected by using univariate techniques, which will result in the loss of efficiency. Another approach is based on the robust estimation of covariance or correlation matrices of the data. Some of the methods used are multivariate trimming (MVT), minimum covariance determinant (MCD) and minimum volume ellipsoid (MVE) (Devlin et. al., 1981). In MVT, a certain percentage of the observations with highest Mahalanobis distance (MD) are removed and the covariance matrix is formed using the remaining observations. In MCD, a subset of data is formed by randomly selecting some percentage of the samples. The determinant of this subset of data is then computed. The mean and S.D. of the data subset with the minimum non-zero determinant are then used to calculate the covariance or correlation matrices. In MVE, the smallest set ellipse, which contains half of the data, is obtained. The mean and S.D. of the samples inside this ellipse are calculated and rescaled so that they estimate a multivariate normal distribution. Such techniques may be suffered with the disadvantage that ignoring the data which are believed to be "good" by process operators will inevitably result the information loss.

In order to maximally use the information provided in the data while lessening the effects of the outliers, other robust approaches have been investigated. In Hybrid projection pursuit (HPP), an M-estimator like formulation is used for weighting each observation in the data set according to its MD so that a weighted PCA is proposed with eliminating the 'discontinuity problems' in projection pursuit (Chen et. al., 1996). However, since HPP relies on the MD, the presence of multiple outliers may yield erroneous results (Hoo, K. A. et. al., 2002). Recently, a method of robust multivariate outlier replacement was developed for PCA modeling (Hoo, K. A. et. al., 2002). In this approach, a winsorization, which is a procedure that replaces the observations by its pseudo values, is carried out iteratively in score space obtained in PCA. The data, especially the outliers, are transformed into a

tight cluster of majority of data set so that the effect of outliers can be reduced. A Huber or Hampel like M-estimator is used in the winsorization process. Even through it is effective in eliminating the outliers, this approach could suffer the performance loss. Because by using Huber or Hampel like estimators, one has to specify the breakdown points, which are the degrees of the freedom in the estimators, and these parameters are difficult to be determined as *a priori*. Injudiciously specified parameters will result in performance loss of the method or erroneous results.

In this article, an adaptive robust PCA method is proposed with the aim of maximal use of the information in the data as well as robustness to the deviation from the ideality caused by the outliers. A winsorization procedure is employed in the score space as that in the approach by Hoo, K.A. et. al., but a partially adaptive M-estimator based on the generalized t (GT) distribution is used instead of Huber or Hampel like estimators. This GT based estimator is obtained directly from the data in score space and its influence curve fit the data adaptively. This will improve the performance and it is optimal in MLE sense. By using GT distribution, the data can adjust itself to the shape of its distribution, in such a way the advantages of both robustness and maximum likelihood estimation (MLE) retained.

The paper is organized as follows. In the next section, a brief overview of robust estimate and several robust estimators are introduced. Specially, robust estimator based on GT distribution and its robust properties are discussed. In section 3, after giving a brief introduction of PCA, the proposed robust PCA approach using adaptive GT based M-estimator is developed. The winsorization procedures of the approach are also highlighted in the section. In section 4, the proposed method is implemented and its performance is compared with that of conventional PCA and the robust PCA using Huber's M-estimator through the data collected from a chemical engineering simulation. Finally, the conclusions are given in the section 5.

2 ROBUST ESTIMATES

2.1 M-estimates

The essence of robust estimates can be explained by the simple one-dimension parameter estimation problem

$$y = f(x, q) + e \tag{1}$$

where y, x and ε are the dependent, independent and error variable, respectively. θ is the parameter to be estimated. After collecting a set of data, the parameter θ can be estimated by least squares method,

$$\hat{\theta} = \arg\min \frac{1}{n} \sum_{i=1}^{n} \left(y_i - f(x_i, \theta)\right)^2 \tag{2}$$

Under the assumption that the error e is normal distributed, the estimation of θ is optimal in the sense of maximum likelihood estimation.

However, if the error is not normal distributed, especially there are outliers in the data, the above estimate will be biased. This problem can be solved by designing a robust estimator, which is insensitive to the deviation of the assumption for the majority of data. The design of this estimator is usually converted into choosing the objective function $\rho(u)$ (not necessary the quadratic one as in the conventional approach) in the optimization problem

$$\hat{\theta} = \arg\min \sum_{i=1}^{n} \rho\left(y_i - f(x_i, \theta)\right) \tag{3}$$

where $\rho(u) = -\ln p(u)$, $p(u)$ is the PDF of the residual $u_i = y_i - f(x_i, \theta)$. Solving the following equations can also solve the above problem,

$$\sum_{i=1}^{n} \psi\left(y_i - f(x_i, \theta)\right) = 0 \tag{4}$$

where $\psi(u) = \rho'(u)$

To be robust, the objective function must give less weight to large value of u than its quadratic form u^2 so that the estimator will down-weight or ignore the contribution of the large errors in the data. In problem (3), a number of candidates $\rho(u)$ can be chosen as the objective function so that different robust estimators can be obtained. These kinds of estimators correspond to the M-estimators in robust statistics. In robust estimation, the ψ function or influence function defined by $\psi(u) = \partial\rho(u)/\partial u$ is the usual tool for comparing alternative M-estimators for their robustness. The ψ function measures the "influence" that a residual will have on the estimation process. Some suggested criteria for the ψ function are that: it is (a) bounded, (b) continuous, and (c) descending and identically zero outside an appropriate region. The motivation for these properties is that (a) a single "anomalous" observation would have limited influence on the estimator, (b) grouping or rounding of data would have minimal impact on the estimator, and (c) ridiculously large observations would have no impact on the estimator.

The typically used robust estimator is Huber's (Huber, 1981)

$$\rho(u) = \begin{cases} \dfrac{u^2}{2} & |u| \le k \\ k|u| - \dfrac{k^2}{2} & k < |u| \end{cases} \tag{5}$$

The influence function is in this case

$$\psi(u) = \begin{cases} -k & u < -k \\ u & -k \le u \le k \\ k & k < u \end{cases} \tag{6}$$

where, k is the parameter characterizing the degree of contamination, being used as tuning parameter for the estimator's performance. Other robust estimators can be found in the literature (Wang, et. al 2000).

Even though the above approaches are less sensitive to gross errors and outliers, the optimality of the estimation, in MLE sense, is still dependent on the suitability of the chosen function with respect to the actual distribution of the data. It is generally hard to characterize the distribution of the errors correctly without posteriori estimation. If the real errors do not follow the specified distributions, the performance of estimator may deteriorate and the estimation could be biased. Considering these disadvantages, a more flexible probability distribution function will be discussed next to describe the error distribution. It is designed to allow for a variety of thickness of tails, to capture the shape of distribution and to accommodate other distribution as much as possible as special cases. The corresponding estimator will then be robust by its ψ function and be efficient by estimating its distributional parameters from the data in the MLE sense.

2.2 The generalized T density and its robust properties

The proposed robust estimator for PCA modeling in this work is based on the assumption that the data in score space is following the generalized T distribution (GT) (Butler, et. al., 1990), which has flexibility to accommodate various distributional shapes

$$f_{GT}(u;\sigma,p,q)=\frac{p}{2\sigma q^{1/2}B(1/p,q)\left(1+\frac{|u|^p}{q\sigma^p}\right)^{q+1/p}} \quad -\infty<u<\infty \tag{7}$$

Where σ, p, q are distributional parameters, σ corresponds to the standard deviation, p and q are parameters corresponding to the shape of distribution. This density is symmetric about zero, uni-modal, and suitable to describe the error characteristics in most cases. By choosing different values of p and q, the GT distribution will accommodate the real shape of the error distribution. The larger the value of p or q, the "thinner" will be the tail of the density. Similarly, smaller values of p and q will be associated with "thicker" tails. The tails behavior and other characteristics of the distribution, depend upon these two distributional parameters, which will be estimated from the data (Wang et. al., 2003). In addition, the GT distribution defines a very general family of density functions and combines two general forms, which include most of stochastic specifications one meets in practice as special or limiting cases.

The robustness of the estimator based on a GT distribution can be discussed by investigating its ψ function. This ψ function, corresponding to the objective function $\rho(u,\sigma,p,q)=-\log f_{GT}(u;,\sigma,p,q))$ is given by

$$\psi_{GT}(u;\sigma,p,q)=\frac{(pq+1)sign(u)|u|^{p-1}}{q\sigma^p+|u|^p} \tag{8}$$

For finite q, this influence function is bounded and reaches a maximum for positive u at $u^*=\left((p-1)q\sigma^p\right)^{1/p}$ and has a maximum value of

$$\psi(u^*;\sigma,p,q)=\frac{(p+1/p)(p-1)^{[(p-1)/p]}}{\sigma q^{1/p}} \tag{9}$$

Furthermore, $\lim_{u\to\infty}\psi(u;\sigma,p,q)=0$, so this influence function exhibits a descending pattern. Consequently, "large" deviation will not have an impact on this estimator when q is finite. Also, for a given finite q, p control the behavior of $\psi(u;\sigma,p,q)$ near the origin. For example, if $p>2$, then this influence function will be less steeply sloped near the origin than the influence function for the t distribution with $2q$ degrees of freedom.

3 PCA AND ITS ROBUSTNESS BASED ON M-ESTIMATE WINSORIZATION

3.1 Principal Component Analysis

The cornerstone of data-driven process monitoring approach is the projection method of PCA. The philosophy of this technique is to reduce the dimensionality of the problem by forming a new set of variables. The method generates the new set of variables, called principal components. Each principal component is a linear combination of the original variables. All the principal components are orthogonal to each other so there is no redundant information. The principal components as a whole form an orthogonal basis for the space of the data. The first few principal components can capture the most of the variance in the data so that they are used as the model. The new data will be fitted by the model in order to see if the measures developed are in the normal range.

Let X be a $n\times m$ data matrix containing n process measurements of m variables $(m\le n)$. PCA decomposes the observation X as

$$X=TP^T=\sum_{i=1}^{m}t_i p_i^T \tag{10}$$

Mathematically, p_i and t_i can be calculated by finding the eigenvalues and their companion eigenvectors of covariance or correlation matrix S of data X,

$$\begin{aligned} S&=P\Lambda P^T \\ T&=XP \end{aligned} \tag{11}$$

where Λ is the diagonal matrix containing the ordered eigenvalues of S and P is the corresponding eigenvector matrix. In PCA, P is defined as loading matrix and T is defined to be the matrix of principal component scores. The loadings provide information as to which variables contribute the most to individual PCs and they are the coefficients on the principal component model; whilst the score matrix provide the information on the clustering of the samples and the identification of transitions between different operating regimes.

In general, if the process variables are collinear, the first k principal components can be used to explain sufficiently the variability in the whole data set with less information loss, and the determination of the number k can be obtained via several techniques such as scree test and cross-validation. It then follows that

$$X = T_k P_k^T + E = \sum_{i=1}^{k} t_i p_i^T + E \tag{12}$$

$$\hat{X} = T_k P_k^T = \sum_{i=1}^{k} t_i p_i^T \tag{13}$$

Once the PCA model is established, analysis and usage of these lower dimension orthogonal variables are preceded and the measures such as T^2 and SPE along with some visualization plots in score space can be employed for process monitoring.

3.2 Robust PCA Based on M-estimate Winsorization

PCA transform the data set by projection onto loading vectors to form score vectors which are uncorrelated. Hence, univariate concepts can be employed in the score space. The outliers present in the original data manifest themselves in the score space. By recurrently winsorizing the scores and replacing them with suitable values, it is possible to detect multivariate outliers and replace them by values, which conform to the correlation structure in the data. The concept of winsorization is briefly explained first and its application to robust PCA is then investigated.

Consider the linear regression problem

$$y = f(X, \theta) + \varepsilon \tag{14}$$

where $y = (y_1, y_2, ..., y_n)'$ is a $n \times 1$ vector of dependent variables, $X = (x_1', x_2', ..., x_n')'$ is a $n \times m$ matrix of independent variables, and θ is a $p \times 1$ vector of parameters, e is a $n \times 1$ vector of model error or residual. An estimation of parameter θ, $\hat{\theta}$, can be obtained by minimizing the function

$$\hat{\theta} = \arg\min \sum_{i=1}^{n} \rho\left(\frac{y_i - f_i(x_i, \theta)}{s} \right) \tag{15}$$

where s is an estimation of the scale of the distribution of residuals and ρ is objective function to be minimized.

With the parameter $\hat{\theta}$ estimated, the prediction or estimation of the dependent variable $y_i \, (i = 1, ..., n)$ is given by

$$\hat{y}_i = f_i(x_i, \hat{\theta}) \tag{16}$$

and the residual is given by

$$r_i = y_i - \hat{y}_i \tag{15}$$

In winsorization process, the variable y_i is transformed using pseudo observation according to specified M-estimates such as Huber's;

$$y_i^w = \begin{cases} \hat{y}_i - k s_i & r_i < -k s_i \\ y_i & |r_i| \le k s_i \\ \hat{y}_i + k s_i & r_i > k s_i \end{cases} \tag{17}$$

here the parameter k is the degree of freedom, which regulate the amount of robustness and s_i is the estimation of scale associated with r_i. Other robust estimates can also be employed, especially the one based on GT distribution:

$$y_i^w = \psi_{GT}(y_i; \sigma, p, q) \tag{18}$$

σ, p, q are the parameters which accommodate the shape of the residual distribution. These parameters can be estimated with the data y_i.

The technique of winsorization can be used in PCA to eliminate the effects of outliers in the following. The data value y in score space can be transformed into a new value y^w by winsorization as follows,

$$y_i^w = \psi(y_i), \qquad i = 1, 2, ...n \tag{19}$$

where y is any robust influence function discussed before. Using the winsorization process, the large values exhibited as outliers in the original data set will be brought closer to the other observations after they are transformed from the score space back to the original data space. A new PCA model is obtained using the new data set. This process is carried out iteratively until there is not much change in the loading vectors.

The advantage of using GT based robust estimate over Huber-like robust estimate is obvious. The GT based approach can accommodate the shape of the residual distribution so that it should be more effective when the winsorization is processed, because the estimate is optimal in MLE sense. Huber-like approach needs to pre-specify the robust parameter in an ad hoc manner, this may result in the inefficiency of the estimation.

The steps of the robust PCA based on GT winsorization are described as follow:

1) Scale the data matrix X^j (j is the iteration number, $j = 1,2,...$) using some estimates of scale and location (μ^j, σ^j). Calculate the correlation matrix S.
2) Apply PCA to the correlation matrix S and generate the PC loadings and scores
3) Fit the score data to the GT distribution and calculate its influence function y . Winsorize the score space variables using the transformation:
$$t_i^{j,w} = \frac{t_i^j + \psi(t_i^j)}{2} \quad i = 1,2,...,n$$
4) Reconstruct the actual data using the loading vector and winsorized score vector,
$$X^{j,w} = T^{j,w} P^{jT} = \sum_{i=1}^{m} t_i^{j,w} p_i^{jT}$$
5) Check for the convergence of the loading vectors, $\max\left(\left\|P^j - P^{j-1}\right\|\right) \le \varepsilon_s$ where ε_s is a user-defined threshold.
6) If convergence is not achieved at iteration j, then go back to step 1, otherwise stop.

4 SIMULATION STUDY

The heat-exchanger network example (Romagnoli and Sanchez, 2000) will be used to demonstrate the performance of the proposed robust PCA modeling method based on GT winsorization (Figure 1).

Process stream A is heated by process streams B, C and D at various junctions. The system has 16 measured variables which are either flow rates or temperatures. The open loop data are generated by adding Gaussian noise with zero mean and variances of 2% of their values on all the values when the process is operating at the normal conditions. 200 samples are generated and the sampling time is 0.1 hour.

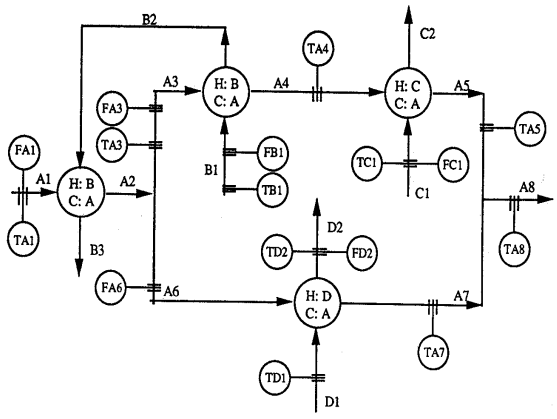

Figure 1 Heat Exchange Network

The data generated above are treated as real good data set and labeled as X^*. In order to compare the performance of the proposed method with the others, outliers are introduced by adding randomly to anywhere in X^* with the larger values (variances up to 10% of their median values) from different error distribution such as Gaussian, *t* and non-central *t* distribution. The case of non-central *t* distribution will be reported here. Figure 2 shows the measurement data corrupted by non-central *t* distribution. This corrupted data set is labeled as X.

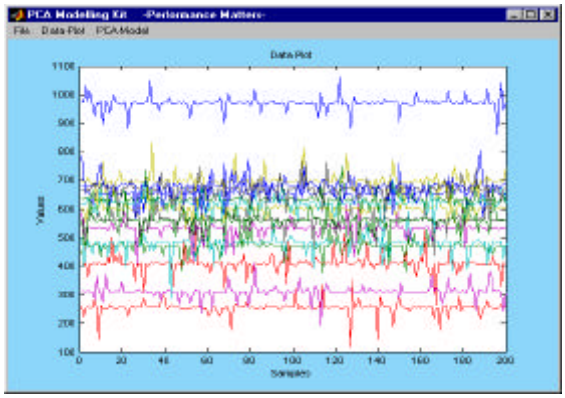

Figure 2 Data Set X

The performance criterion which will be used to compare the efficiencies of the various PCA methods is the mean-squared error (MSE):

$$\text{MSE} = \frac{1}{m}\sum_{i=1}^{m}\left(\lambda_i^* - \lambda_i\right)^2 \qquad (20)$$

where, is the eigenvalue vector of data matrix , is the eigenvalue vector of reconstructed data matrix by different PCA approaches with corrupted data , is the dimension of the variables or the number of principal components chosen. The MSE is constructed such that better performance is obtained if its value is driven toward zero.

Figure 3 shows the normal plot of the data . If the data fell on the straight lines, then their distribution is assumed to be normal. Clearly, it shows that the data are not normal distributed.

Three PCA methods are applied to the data , the results are shown in the tables. Table 1 lists the explained variation in the data by each eigenvalue along with the cumulative percentage of the explained variation. If the selection of the number of principal components is based on a requirement that 85% of the variance be explained, then eight principal components are required for original data. However, for the same criterion seven principal components are required based on the conventional PCA with the corrupted data . The robust PCA approaches can recover the real variation explained by the principal components so that they diminish the effects of outliers in the data. The proposed GT based winsorization has better performance than the winsorization

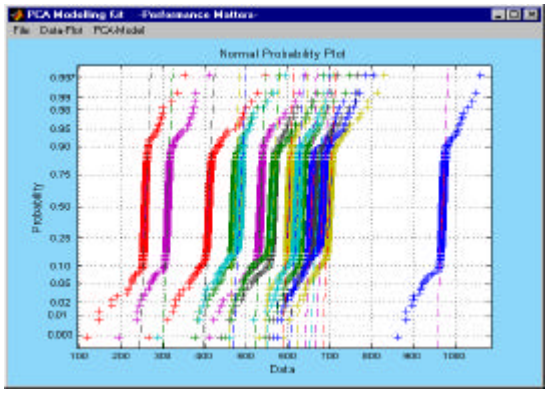

Figure 3 Normal Plot of Data

using Huber estimator. This is due to that GT winsorization can accommodates the distribution of the data, while winsorization based on Huber estimator relies on *a priori* parameters so that it is not adaptive. Judiciously specifying the threshold in Huber-like winsorization may improve the performance. The normal plots of the filtered data are given in Figure 4. It is shown that after the winsorization based on the GT, the distributions of the data are normal so the correct results can be obtained by using PCA with the data X. The MSE criterion is listed in table 2, which shows that the proposed approach has the best performance. It is also observed in table 1 that for the outliers-free case, the proposed robust PCA approaches still have acceptable performance.

5 CONCLUSIONS

A Robust PCA modeling method based on winsorization in score space using adaptive robust estimator was developed and presented. The effects of outliers in the data can be eliminated by the method while the effectiveness as well as the robustness is kept by using GT-like estimator. The performance of the proposed method is compared with the others using a chemical example. The usage of the approach in process monitoring such as faults detection, identification and diagnosis is promising.

6 REFERENCES

Butler, R. J., McDonald, J. B., Nelson, R D., White, S. B.(1990), "Robust and Partially Adaptive Estimation of Regression Models", The Review of Economics and Statistics, 1990, 321

Chen, J., A. Bandoni and J. A. Romagnoli (1996), "Robst PCA and Normal region in multivariate statistical process monitoring", AIChE. J. 42(12), 3563-3566

Devlin S. J., Guanadesikan, R. and Kettenring, J. R. (1981), "Robust Estimation of Dispersion matrices and principal components", J. of Amer. Stats. Asso. 76, 354-362

Hoo. K.A., K.J. Tvarlapati, M.J. .Piovoso and R. Hajare, (2002) "Amethod of robust maultivariate outliers replacement", Comp. Chem. Eng. 26. 17-39

Huber, P. J., (1981), "Robust Statistics", *John Wiley & Sons, New York, NY.*

Kresta, J. V. J. F. MacGregor and T. E. Marlin (1991), "Multivariate statistical monitoring of process operations", Can. J. of Chem. Eng., 69, 35.

Romagnoli, J. A. and M, C. Sanchez, (2000), "Data Processing and Reconciliation for Chemica Process Operations", *Academic Press.*

Wang, D., Safavi A. and Romagnoli J. A., (2000), "Wavelet-based adaptive robust M-estimator for nonlinear systems identification", AIChE Journal, 46, 8. 1607-1615.

Wang, D. and Romagnoli, J. A. (2003), "A Framework of Robust Data Reconciliation Based on a Generalized Objective Function", to appear on J. of Industrial and Engineering Chemistry Research.

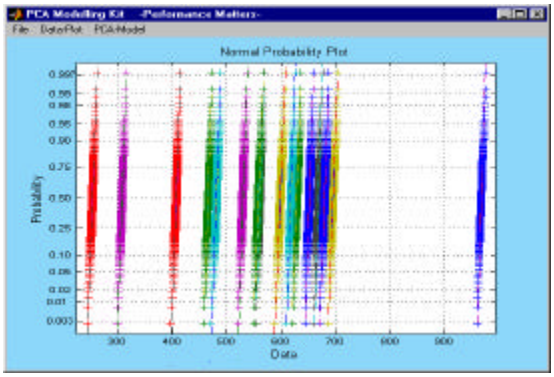

Figure 4 Normal Plot Data after Winsorization

Table 1. Results of PCA

Num. of PCs	Explained variance(%) Data X^*	Cumulative explained variances(%)	Explained variance(%) X	Cumulative explained variances(%)
	conventional			
1	17.6918	17.6918	21.3087	21.3087
2	16.1712	33.8630	16.2429	37.5515
3	15.6300	49.4930	14.5289	52.0805
4	10.0487	59.5417	11.9913	64.0718
5	9.2196	68.7613	9.3763	73.4482
6	8.3142	77.0755	6.9700	80.4182
7	6.7640	83.8395	5.4210	85.8392
8	5.4261	89.2656	4.3469	90.1862
	Huber's			
1	18.7511	18.7511	19.3563	19.3563
2	17.1491	35.9002	15.3889	34.7452
3	11.8246	47.7249	11.6123	46.3576
4	10.2274	57.9523	10.8261	57.1837
5	9.2651	67.2174	9.2336	66.4173
6	7.5333	74.7507	7.6582	74.0755
7	6.0656	80.8163	6.7601	80.8356
8	4.7430	85.5593	5.9184	86.7540
	GT			
1	17.2848	17.2848	17.3761	17.3761
2	16.4029	33.6877	14.3915	31.7676
3	13.0628	46.7505	14.2124	45.9801
4	10.2440	56.9946	11.4886	57.4687
5	9.2602	66.2548	9.3367	66.8054
6	7.3126	73.5674	8.1144	74.9198
7	6.9677	80.5351	6.6013	81.5211
8	6.1711	86.7062	5.1630	86.6841

Table 2. MSE values of different methods

	Conventional PCA	Huber's Winsorization	GT Winsorization
MSE	4.7826	2.6002	0.9374

A FRAMEWORK FOR ON-LINE TREND EXTRACTION AND FAULT DIAGNOSIS

Mano Ram Maurya [*] **Raghunathan Rengaswamy** [**]
Venkat Venkatasubramanian [*,1]

[*] *Laboratory for Intelligent Process Systems, School of Chemical Engineering, Purdue University, West Lafayette, IN 47907, USA.*
[**] *Department of Chemical Engineering, Clarkson University, Potsdam, NY 13699-5705, USA.*

Abstract: Qualitative trend analysis (QTA) is a process-history-based data-driven technique that works by extracting important features (trends) from the measured signals and evaluating the trends. QTA has been widely used for process fault detection and diagnosis. Recently, Dash *et al.* (2001, 2003) presented an interval-halving-based algorithm for off-line automatic trend extraction from a record of data, a fuzzy-logic based methodology for trend-matching and a fuzzy-rule-based framework for fault diagnosis (FD). In this article, an algorithm for on-line extraction of qualitative trends is proposed. A framework for on-line fault diagnosis using QTA also has been presented. Some of the issues addressed are - (i) development of a robust and computationally efficient QTA-knowledge-base, (ii) fault detection, (iii) estimation of the fault occurrence time, (iv) on-line trend-matching and (v) updating the QTA-knowledge-base when a novel fault is diagnosed manually. Some results for FD of the Tennessee Eastman (TE) process using the developed framework are presented.

Keywords: Qualitative Trend Analysis, On-Line, Fault Detection, Fault Diagnosis.

1. INTRODUCTION

Modern plants are data rich and information poor. Vast amount of process data is available which can be used to assess the process state by utilizing the important features present in the measured data. Qualitative trends (e.g. increasing, constant etc.) are the most natural representation of features that have been widely used for FD. Every diagnostic system that uses process trends to achieve fault classification has three components: (i) a language for trend representation such as triangular episodes (Cheung and Stephanopoulos, 1990), primitive-based language (Janusz and Venkatasubramanian, 1991) and piecewise-linear elements (Mah *et al.*, 1992), (ii) a methodology to extract the trends such as wavelet-based method (Bakshi and Stephanopoulos, 1994*a*), use of wavelet, neural networks and B-Splines-based method (Vedam, 1999) and (iii) a classification methodology and a knowledge-base to map the sensor-trends into faults such as decision trees (Bakshi and Stephanopoulos, 1994*b*), weighted symptom trees (WST) (Oh *et al.*, 1997) and fault or sensor centric trees (Vedam, 1999). Recently Dash *et al.* (2001) proposed an interval-halving-based algorithm for automatic trend extraction. The primitive-based language (Janusz and Venkatasubramanian, 1991) is used for the representation of the qualitative trends. The seven primitives, *viz.* A(0, 0), B(+, +), C(+, 0), D(+,

[1] Author to whom all correspondences should be addressed, E-mail: venkat@ecn.purdue.edu, phone: (765) 494 0734, fax: (765) 494 0805.

-), E(-, +), F(-, 0), G(-, -) where the signs are of the first and second derivatives, respectively, are shown in Figure 1. The primitives B, D, E and G are nonlinear primitives. Dash *et al.* (2003) also developed a fuzzy-logic-based framework for trend-matching and fault diagnosis. The overall activity of trend-extraction and trend-matching is called qualitative trend analysis (QTA).

While the interval-halving algorithm, the trend-matching methodology and their application for FD have been discussed in detail (Dash *et al.*, 2001; Dash *et al.*, 2003), on-line implementation has not been discussed. Though the research work by Vedam (1999) dealt with some of the issues involved in on-line implementation of trend-similarity-based FD, little has been discussed in the published literature. In this article, we discuss most of the important issues that are involved in on-line fault diagnosis. In particular, we present an algorithm for on-line trend extraction using the interval-halving technique to achieve computational efficiency and robustness. A framework for on-line FD using QTA is also presented. The organization of this article is as follows.

In the next section, an overview of QTA is presented. In section 3, we motivate the need for an on-line variant of the interval-halving algorithm and discuss some of the challenges. We also list the activities that are carried out in on-line FD using QTA. In section 4, the design of the algorithm for the on-line variant is discussed. The framework for on-line FD is discussed in sections 5 and 6. Section 5 deals with development of a knowledge-base (KB) for QTA. Section 6 deals with the use of the QTA-KB for on-line FD. In section 7, a succinct discussion on the development of a prototype diagnostic system in Matlab® is presented. Sample results of FD in the TE process are also presented. Finally we conclude this article with discussion on future work.

2. OVERVIEW OF QTA

There are two subtasks in QTA- (i) trend extraction (Dash *et al.*, 2001) and (ii) trend matching (Dash *et al.*, 2003). A brief discussion follows.

Trend extraction by using the interval-halving algorithm: The algorithm works by fitting either a constant, a first order or a second order polynomial (in that order) to the data and halving the interval if the fit error is significant as compared to the noise present in the signal (as dictated by the F-test) even for the quadratic function. Once the polynomial is fitted over a certain interval, a primitive is assigned based upon the sign of the first and second derivatives (t-test is used to check the significance of the derivatives).

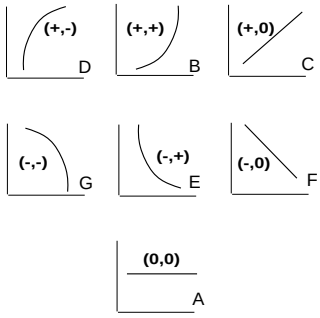

Fig. 1. Fundamental language: primitives

Then the interval-halving procedure is applied to the remaining data till the entire signal is transformed into a sequence of primitives.

Fuzzy trend-matching: Trend-matching involves calculation of the following: (a) fuzzy similarity match between two primitives, (b) similarity measure between two trends (the time-weighted average of the similarity match between the primitives involved in different time intervals) for the same sensor and (c) multivariate (overall) similarity measure or confidence index (C.I.) between two scenarios (given by $C.I. = min(S_1,\ S_2,\ \ldots,\ S_n)$ where n is the number of sensors and S_k is the similarity measure between the trends of the k^{th} sensors in the two scenarios). To perform fault diagnosis by using QTA, the faults stored in the QTA-KB are rank ordered in decreasing order of their C.I. The fault with the highest C.I. is the fault that has most likely occurred. A low value of C.I. (say below 0.50) for all the faults indicates the occurrence of a novel fault.

3. ON-LINE FAULT DIAGNOSIS USING QTA: MOTIVATION AND ISSUES

Our ultimate aim is to implement the QTA-based fault diagnosis in real plants. In off-line trend extraction, the interval halving algorithm is applied on the entire data. During on-line implementation, more and more data is available from sensor measurements. The primitives obtained at current time may no longer correctly represent the trend at a future time. Thus a key feature of an algorithm for on-line trend extraction is that the primitives should be updated as more data becomes available. On one hand, trend extraction cannot be performed on all the data available so far at every sample time. On the other hand, if one were to find trends corresponding to only the new data, one would end up assigning only 'A' primitives since no useful trend is contained in few samples. Thus the data set for trend extraction should comprise of some of the past data and the newly available data. This poses the question of how should one choose the data segment for trend extraction? Some related questions are- (i)

should the data segments chosen for two consecutive trend extractions overlap?, (ii) can one calculate an average primitive in the overlapping region?, etc. These issues are discussed in the next section. Further, for real-time FD, we need to consider the following- (i) building a knowledge-base of fault-symptom signatures, (ii) detecting the occurrence of an abnormal event (fault detection), (iii) extracting the relevant portion of trend from an arbitrarily long sequence of primitives (does fault occurrence time play a vital role?), (iv) time-efficient computation of similarity measure and (v) learning- updating the QTA-KB if a novel fault is manually diagnosed by the operator. Discussion on on-line trend extraction follows.

4. ON-LINE TREND EXTRACTION

Given sensor data, the basic interval-halving algorithm can be applied on the entire data in off-line fashion to extract trends. From the above discussion it is clear that the trend extraction has to be performed over a window of data, that the window should move as more data becomes available and that the trend extracted in the current window has to be intelligently combined with the already extracted trends. Before trying to device an algorithm to carry out additional preprocessing (and possibly post-processing) for on-line trend extraction, let us briefly analyze the off-line and on-line implementation of another methodology for trend-extraction *viz.* B-Spline based trend extraction (Vedam, 1999).

To implement the B-Spline based algorithm (which extracts linear primitives) for on-line trend extraction by using a sliding-window approach, off-line algorithm is applied on a window containing 2^k+1 samples (k is a positive integer). After measuring p more samples, the window slides by p data points (the window size does not change). This is similar to the sliding window approach for on-line denoising using wavelet analysis. Now to get a consolidated list of linear primitives till the current time, the primitives in the current window are combined with the old list of consolidated linear primitives. Since the primitives to be combined are linear, an average value can be used at the starting point of the current window. After this time instant, the old primitives are replaced by the primitives in the current window. Every time trends are extracted, after updating the list of linear primitives, they are concatenated to get higher order primitives. The higher order primitives are not updated directly. Now let us analyze the key features of the off-line interval-halving algorithm for trend extraction.

The basic interval-halving algorithm is capable of extracting nonlinear primitives directly and no concatenation is needed. This means that if the interval-halving algorithm identifies a nonlinear primitive then there is no need to allow this nonlinear primitive to evolve further except when the primitive length is very small. This is a very good feature since concatenation requires a parameter (magnitude threshold) for every sensor and is not transparent.

Given that one should preserve the ability to extract nonlinear primitives and avoid concatenation, unlike on-line implementation of B-Spline based methodology, averaging at the starting point of the current window is not an option. In fact, averaging would render the polynomial coefficients (which can be used for data compression) useless. Similarly, concatenation is not allowed. Yet, the primitives should evolve as more data comes in. Two key ideas to achieve this effect are explained below.

Unrestricted evolution of the last primitive of the current window: By the nature of the interval-halving algorithm, as more samples are available, only the last primitive evolves. This assumption may be violated for very small time intervals (where one of the primitives before the last primitive could be an 'A' primitive) due to parameter-less and 'fit the simplest-primitive' nature of the algorithm. Such local violations do not have much effect on similarity measure.

If the last primitive is a linear primitive ('A', 'C' or 'F') then allow it to evolve until it becomes a nonlinear primitive or it becomes very long (so that further evolution would require too much computation). If the last primitive is a nonlinear primitive then it should not be allowed to evolve except when its length is too small.

Parameters and selection of the window: Three important parameters are the default window length, the length of the shortest primitive (minNLP_len) and the length of the longest linear primitive (maxCFlen). For choosing the window, the endpoint of the current window should coincide with the last sample available. The starting point of the window can be chosen to coincide with the starting point of the last primitive. With this rule in effect, the window size changes adaptively. One exception to this rule is that if the last primitive is nonlinear and is very long then one can choose the starting point of the window so as to keep the window size equal to the default window size. Depending upon how window is selected, one should keep a record of the primitives that would not evolve anymore so that the most updated list of primitives can be obtained simply by appending the primitives in the current (or latest) window to the existing list of non-evolving primitives. The above procedure of window selection is schematically shown in Figure 2. A flowchart for the overall

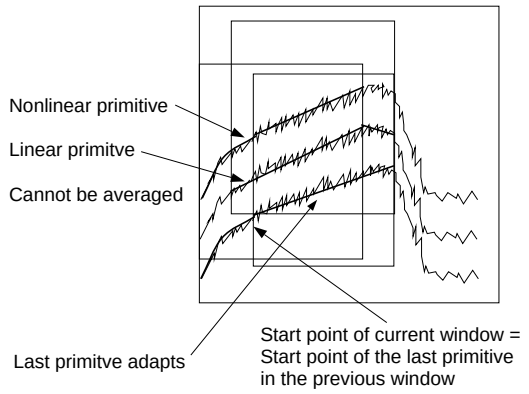

Fig. 2. Adaptive selection of the window

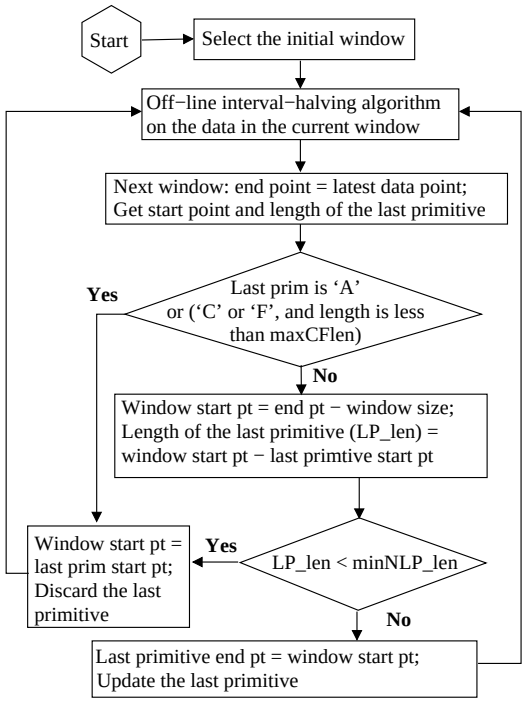

Fig. 3. Flowchart for on-line trend-extraction

algorithm is shown in Figure 3. Figure 4 shows a snapshot of trend-extraction in two consecutive windows for a sample signal. If one were to use the interval-halving algorithm on a sliding window of fixed length (65), the last primitive (at the current time) would still have been 'A'. Also, unnecessary computation would have been performed over a certain portion of the first primitive.

5. BUILDING QTA KNOWLEDGE-BASE

Development of the QTA-KB primarily involves trend-extraction for all known faults. Some of the parameters (which are universal for a given plant) related to QTA-KB are- description of the faults stored (including whether the fault truly corresponds to an abnormal scenario), description of the sensors which are used for trend extraction *viz.* sample rate, normal value, noise etc., the start and endpoints of the data used for trend

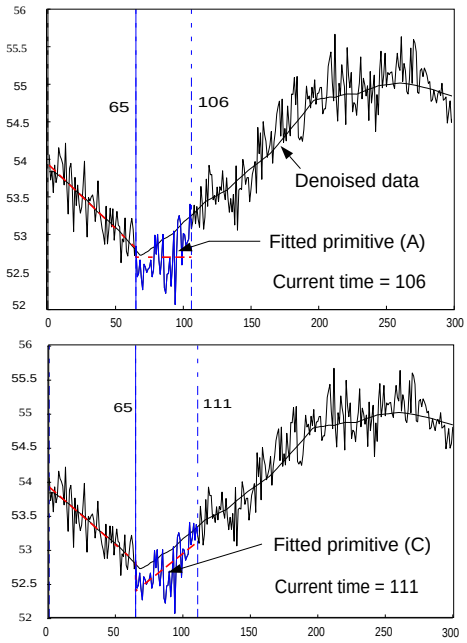

Fig. 4. Snapshots during two consecutive windows

extraction for each sensor in every fault scenario, the global parameters related to on-line trend extraction such as default window length etc. For small-scale plants, where the number of sensors is small (say, less than 100), one may be able to compute similarity measure for all the sensors with all the fault scenarios in real-time but for large plants, it may be infeasible. For large plants, one must consider the issue of computational complexity. Apart from computational infeasibility, it is expected that the sensors that are physically located near the fault origin would show departure from their normal operating region (NOR) before the sensors that are located far away. Hence, such sensors are useful in detecting the fault occurrence and they should be chosen for estimating the similarity measure. Thus optimal selection of sensors (that should be used for calculation of similarity measure) corresponding to each fault is very important. Other issues in optimal selection of sensors are- (i) consistency among similar faults: the sensors should show similar trends for multiple manifestations of the same fault and (ii) discrimination from other faults: the sensors should be chosen so that they provide maximum discrimination from other (different) faults. These ideas have been earlier discussed and implemented by Vedam (1999). Further, when lesser (but sufficient) number of sensors are chosen, most likely the chosen sensor would show fast evolution. This would result in robustness in the calculation of similarity measure, particularly during the incipient stage of fault evolution, the duration in which one is interested in diagnosing the fault. Since the confidence index assigned to a fault is the minimum of the similarity measure for the sensors dedicated to diagnose the fault, if all the sensors

are chosen blindly for assessing every fault then correct diagnosis would be delayed. To summarize these ideas, the sensors dedicated for diagnosing various faults should be chosen with respect to three criteria: (i) consistency among similar faults, (ii) fast dynamics for the fault and (iii) discrimination from other faults. The procedure for optimal screening of sensors is discussed below-
[1] Extract trends for all the sensors for all the fault scenarios.
[2] Compute a global similarity matrix containing the similarity measure for each sensor for all pairs of faults. Perform the steps 3-7 for every fault.
[3] Identify the set of faults that are similar to this fault, and the set of faults that are different.
[4] Corresponding to the set of similar faults, for each sensor, extract the similarity measures from the similarity matrix and take the minimum. Rank the sensors in decreasing order of the minimum. Thus the sensor that shows maximum similarity would be on the top of the list (list 1).
[5] Corresponding to the pairs of this fault with the different faults, extract the similarity measures for all sensors, take the maximum for each sensor, and rank the sensors in increasing order of the maximum. Thus the sensors that shows least similarity measure (maximum discrimination) would be on the top of this list (list 2).
[6] Rank the sensors in decreasing order of speed of evolution (the sensor that evolves the fastest should be on the top) (list 3).
[7] Prepare a new list by selecting sensors from list 1 and list 3 (rank them according to a weighted criterion). This new list is a ranked list of sensors in decreasing order of consistency and speed of evolution. If the value of the weighted criterion is equal for two or more sensors in this list then sort them according to list 2 (decreasing discrimination). Now select sensors from the new list one after another till the fault can be resolved from all other (different) faults.

Of course, in the above procedure, a fail-safe approach should be adopted so that sufficient number of sensors are chosen to ensure discrimination from other faults. In some rare cases, where the data used for developing the knowledge-base is not collected properly, consistency with similar faults and discrimination from different faults could be in conflict. In such cases, a robust and reliable knowledge-base cannot be developed.

6. ON-LINE FAULT DIAGNOSIS

During online implementation, the primitives are continuously extracted. When a fault occurs, the sensors start deviating from their normal values. Thus the first step is fault detection. In QTA-based fault detection, the presence of a non-

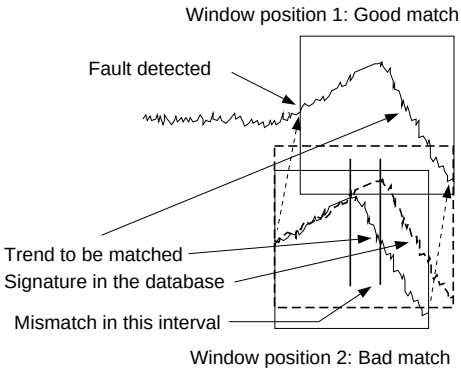

Fig. 5. Importance of fault occurrence time

A primitive and departure from the NOR indicates presence of a fault. A suitable multivariate methodology also can be used for fault detection. After detection, it is very important to estimate the time at which the fault occurred so that an appropriate portion from the infinite sequence of primitives can be extracted. If the fault occurrence time is not estimated properly then poor similarity measure may be obtained (see Figure 5) even for very similar trends. Due to excessive computational complexity, similarity measures with shifted trends cannot be evaluated in real-time and hence, good estimate of fault occurrence time is required. The methodology used for the estimation of the fault occurrence time is called *backtracking*. As shown in Figure 6, once a fault is detected, we try to fit an 'A' primitive in the last interval. If an 'A' can be fitted then there is little variation which means that the fault occurred sometime before this interval. So the estimation window is stretched backwards and this procedure is repeated over the stretched window till an 'A' primitive cannot be fitted *i.e.* there is enough variation in the data in the estimation window. This procedure always terminates since last primitive is a non-A primitive. Trends are recalculated for the data after the fault occurrence time. It can be seen that this method does not take into account the time-delay but that is not a problem because, to ensure robust estimation of similarity measure, the same methodology can be used during the development of the QTA-KB. As the fault evolves, more and more sensors deviate from their NOR. These sensors are used for the estimation of similarity measure and C.I. for various faults. This ensures that similarity measure for a slowly evolving sensor or a sensor that is not showing enough deviation would not result in incorrect C.I. for the actual fault. To summarize, the main activities involved in on-line FD are:

- *Fault detection*
- *Estimation of the fault occurrence time*
- *Computationally efficient trend matching*
- *Learning and updating the QTA-KB*

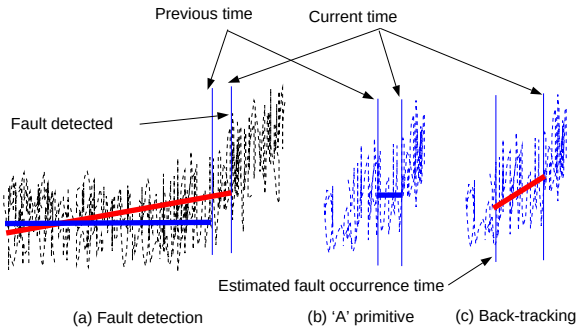

Fig. 6. Estimation of the fault occurrence time

7. A PROTOTYPE DIAGNOSTIC SYSTEM

A prototype diagnostic system to implement the framework discussed above has been designed in Matlab®. To give a brief idea about the important features of the framework, some of the components are succinctly discussed below:

Development of QTA-KB: Trends for various fault scenarios are extracted and sensors to be used for estimating the C.I. for various faults are identified.
On-line trend extraction: The adaptive trend-extraction algorithm is used.
Fault detection: Presence of a fault is triggered if a sensor deviates from its NOR and shows a non-A primitive.
Fault occurrence time: Backtracking methodology is used. The relevant trends are re-calculated.
Fault diagnosis: C.I. for various faults are calculated. The operator is informed about the abnormal sensors and the known or an unknown event.
Learning and updating the QTA-KB: If a novel event occurs and the operator diagnoses the fault, it is added to the QTA-KB.

The diagnostic system has been tested on the TE process (sample time is 0.001 hr for all 14 sensors). No optimal sensor assignment has been carried out for this case study. Out of the 33 possible faults, 26 faults are used to build the QTA-KB. Results for three test scenarios are as follows:

(1) Fault 1: correct diagnosis.
(2) Fault 25: faults 17, 25 and 18 (located in the same control loop).
(3) Fault 28 (novel fault): fault 20 (located in the same control loop as fault 28).

Thus the prototype diagnostic system is quite robust with respect to correct FD and detection of novel events. Interaction with the operator, learning and maintenance is also easily facilitated. Another important characteristic of the overall approach is that most of the parameters used can be easily tuned and that reasonable variation in them does not degrade the overall performance. For example, in the TE process, characteristic time is few hours. The normal window size is 255 ($1/4^{th}$ of the number of samples per hour). maxCFlen and minNLP_len are 1000 and 50, respectively. The window shift length is 15 (to allow the necessary computations every minute).

8. CONCLUSIONS AND FUTURE SCOPE

Various issues in on-line trend extraction and fault diagnosis have been discussed. An algorithm for the same has been presented. A framework for on-line fault diagnosis has been presented. Important components have been discussed. A prototype for FD has been developed in Matlab®. Some results for FD of the TE process have been discussed. Our future work will include improvement in on-line trend extraction (to further reduce computation time) and multiple fault diagnosis.

REFERENCES

Bakshi, B. R. and G. Stephanopoulos (1994*a*). Representation of process trends – III. Multi-scale extraction of trends from process data. *Comput. & Chem. Engng.* **18**(4), 267–302.

Bakshi, B. R. and G. Stephanopoulos (1994*b*). Representation of process trends – IV. Induction of real-time patterns from operating data for diagnosis and supervisory control. *Comput. & Chem. Engng.* **18**(4), 303–332.

Cheung, J. T. and G. Stephanopoulos (1990). Representation of process trends – Part I. A formal representation framework. *Comput. & Chem. Engng.* **14**(4/5), 495–510.

Dash, S., R. Rengaswamy and V. Venkatasubramanian (2001). A novel interval halving algorithm for process trend identification. In: 4^{th} *IFAC Workshop on On-Line Fault Detection & Supervision in the Chemical Process Industries, Korea.* pp. 155–160.

Dash, S., R. Rengaswamy and V. Venkatasubramanian (2003). Fuzzy-logic based trend classification for fault diagnosis of chemical processes. *Comp. & Chem. Eng.* **27**(3), 347–362.

Janusz, M. and V. Venkatasubramanian (1991). Automatic generation of qualitative description of process trends for fault detection and diagnosis. *Engng Applic. Artif. Intell.* **4**(5), 329–339.

Mah, R. S. H., A. C. Tamhane, S. H. Tung and A. N. Patel (1992). Process trending with piecewise linear smoothing. *Comput. & Chem. Engng.* **19**(2), 129–137.

Oh, Y. S., K. J. Moo, E. S. Yoon and J. H. Yoon (1997). Fault diagnosis based on weighted symptom tree and pattern matching. *Ind. Eng. Chem. Res.* **36**, 2672–2678.

Vedam, H. (1999). OP-AIDE: An intelligent operator decision support system for diagnosis and assessment of abnormal situations in process plants. PhD thesis. Purdue University.